

**EFFECT OF TOOL ROTATION IN MECHANICAL &
MATERIAL BEHAVIOUR OF FRICTION STIR WELDED (FSW)
DISSIMILAR ALUMINIUM ALLOYS: AA 6061 & AA 6063**

A Thesis Submitted in Partial Fulfillment of the Requirement

For The Award of the Degree Of

**MASTER OF ENGINEERING IN
MECHANICAL ENGINEERING**

In the

FACULTY OF ENGINEERING AND TECHNOLOGY,

JADAVPUR UNIVERSITY

Submitted by

SUVASIS MUKHERJEE

Class Roll No. 002111202025

Exam Roll No. M4MEC23011

Under the guidance of

Prof Abhishek Mondal (JU) & Dr. Sumata Bagui (CSIR-NML)

DEPARTMENT OF MECHANICAL ENGINEERING

**JADAVPUR UNIVERSITY
KOLKATA-700032, INDIA
2023**

**JADAVPUR UNIVERSITY
FACULTY OF ENGINEERING AND TECHNOLOGY**

CERTIFICATE OF RECOMMENDATION

This is to certify that Mr. **SUVASIS MUKHERJEE** has completed his thesis entitled “**Effect of Tool Rotation in Mechanical & Material Behaviour of Friction Stir Welded (FSW) Dissimilar Aluminum Alloys : AA 6061 & AA 6063**” under the supervision and guidance of **Prof. Abhishek Mandal – Jadavpur University Kolkata & Dr Sumanta Bagui -CSIR NML Jamshedpur INDIA**. We are satisfied with his work, which is being presented for the partial fulfillment of the degree of **Master of Engineering in Mechanical Engineering, Jadavpur University Kolkata - 700032**.

Prof. Abhishek Mandal
Thesis Advisor

Assistant Professor Dept. of Mechanical Engineering
Jadavpur University, Kolkata-700032

Dr. Sumanta Bagui
Thesis Advisor

Principal Scientist
Materials Engineering Division
CSIR-National Metallurgical Laboratory
Jamshedpur - 831007, Jharkhand, India

HEAD, Dept. of Mechanical Engineering
Jadavpur University, Kolkata-700032

DEAN, Faculty of Engineering and Technology
Jadavpur University, Kolkata-700032

**JADAVPUR UNIVERSITY
FACULTY OF ENGINEERING AND TECHNOLOGY**

CERTIFICATE OF APPROVAL*

The foregoing thesis is hereby approved as a creditable study of an engineering subject carried out and presented in a manner of satisfactory to warrant its acceptance as a pre-requisite to the degree for which it has been submitted. It is understood that by this approval, the undersigned does not necessarily endorse or approve any statement made, opinion expressed, and conclusion drawn therein but the thesis only for the purpose for which it has been submitted.

Final Examination for
Evaluation of the Thesis

Signature of Examiners

* Only in case the thesis is approved.

Dedicated to

My Family members:

My Son – Souparno Mukherjee

My Wife - Mrs. Debolika Mukherjee

My Mother- Mrs. Mandira Mukherjee

My Father – Mr. Rabindra Nath Mukherjee

*Because they believe in me, whatever I am doing that is good for us
that's why every time their trust motivate me to work hard and honestly*

ACKNOWLEDGEMENT

First and foremost, I'd like to convey my sincere admiration and appreciation to my advisors and mentors, **Prof Abhishek Mandal, Jadavpur University and Dr. Sumanta Bagui, CSIR NML** who have been the driving force behind this work. I owe him a huge debt of gratitude for his unwavering support, invaluable advice, and for pulling me forward in every aspect of my academic career. His presence and excitement have had a significant impact on my work and vision for the future. I consider it a blessing to be able to work with such a wonderful person.

I'd also like to take this opportunity to thank all of the faculty members in the Mechanical Engineering department for their mental support, invaluable assistance, and cooperation throughout the course of this thesis work.

I'd like to express my gratitude to Jadavpur University Technical Staff **Mr. Jayanta Bhattacharya** for his continuous academic support throughout the thesis work, without which it would not have been completed successfully.

My sincere gratitude goes out to my friends and classmates for their invaluable assistance, cooperation, and support. I enjoyed their companionship so much during my stay at Jadavpur University, Kolkata.

I am especially indebted to my wife and Son, **Mrs. Debolika Mukherjee**, and "**Little Master**" **Souparno Mukherjee** their love, sacrifice, and support towards my education. for their support at various stages of the thesis work.

.....
Suvasis Mukherjee
Class Roll No. 002111202025
Exam Roll No.M4MEC23011

TABLE OF CONTENTS

<i>CHAPTER 1:</i> INTRODUCTION	Page 1-16
<i>CHAPTER 2:</i> LITERATURE REVIEW AND RESEARCH REVIEW	Page 17-19
OBJECTIVE & SCOPE OF PRESENT WORK	Page 20-21
<i>CHAPTER 3:</i> EXPERIMENT'S USED	Page 22-31
<i>CHAPTER 4:</i> EXPERIMENTAL PROCEDURES	Page 32-43
<i>CHAPTER 5:</i> RESULTS AND DISCUSSION	Page 44-72
<i>CHAPTER 6:</i> CONCLUSION AND FUTURE SCOPE OF WORK	Page 73-75
<i>REFERENCES</i>	Page 76-77

CHAPTER -1

INTRODUCTION

1.01 Metal Joining:

Metal joining is a way of combining two or more materials via an external mechanism. Because conventional manufacturing methods such as casting, forging, rolling, extrusion, and so on cannot produce large or sophisticated work piece designs, there is a high demand for metal joining. As illustrated in Figure 1.1, there are numerous methods for joining materials.

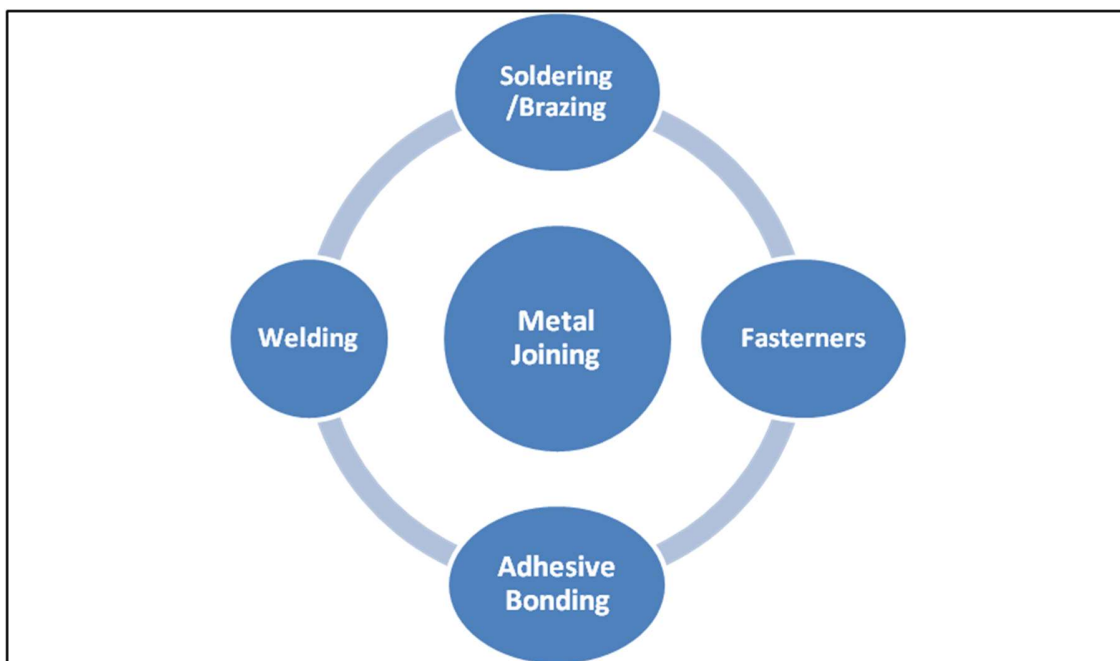


Figure 1.1: Various t Method of Metal Joining [1]

1.02 Welding:

Welding is a joining method that causes coalescence to combine materials, typically metals or thermoplastics. Welding is a critical and frequently utilized manufacturing procedure in all manufacturing/production businesses. The primary goal of welding technique is to provide the best possible condition for a defect-free junction. There are primarily two forms of welding:

Fusion welding and solid-state welding are two types of welding. In fusion welding, a heat source is used to melt the material, and then pressure is used to combine the materials, whereas solid state

welding, such as friction stir welding (FSW), is done below the melting temperature of the work piece. Figure 1.2 displays several welding techniques.

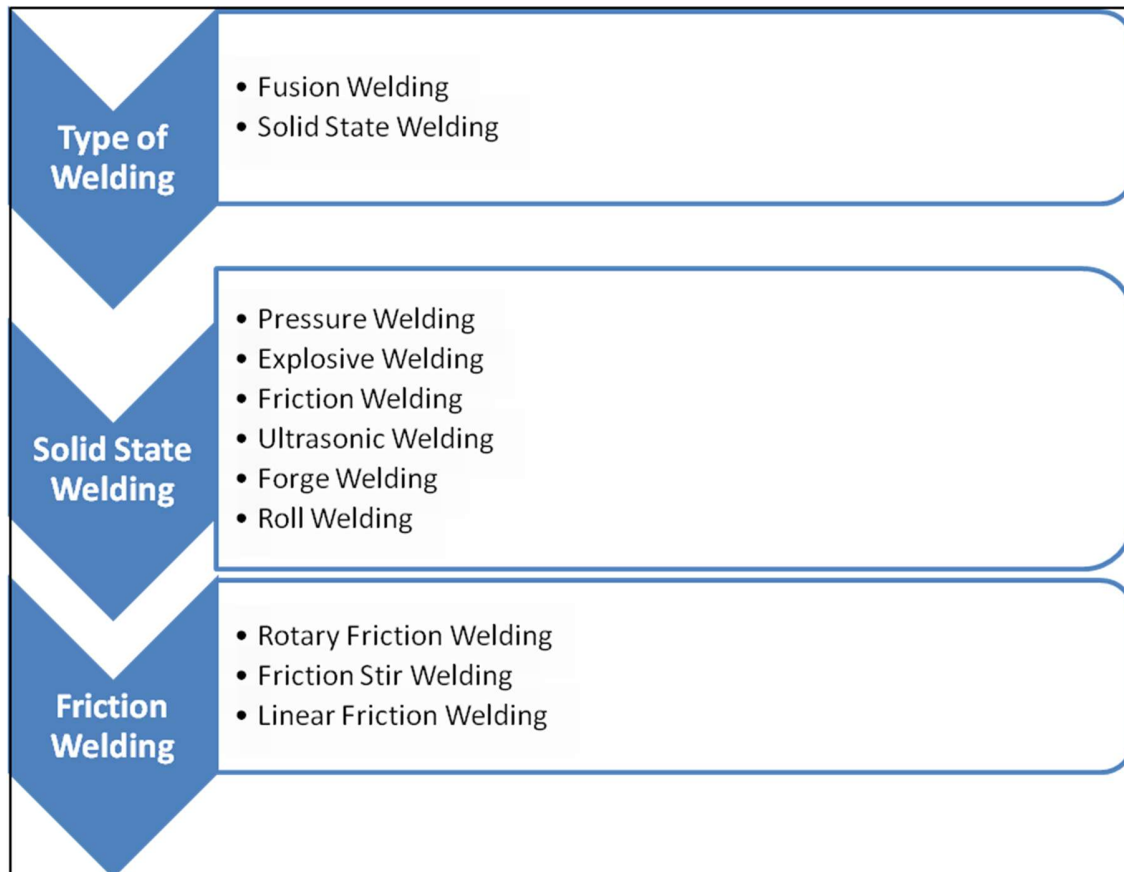


Figure 1.2: Flow chart of welding process [2]

There are several general issues with fusion welding, including [3,4]:

- Mechanical qualities deteriorate owing to melting and re-solidification.
- Extensive consumable filler material is required.
- Flux application and shielding gas utilization.
- Energy use is excessive.
- Flue gas pollution causes environmental issues.

Certainly, solid state welding is superior to fusion welding for the reasons stated above.

Because my M. Enggthesis work is on Friction stir welding (FSW), a solid-state welding method, FSW will only be discussed in detail from now on.

1.03 Friction Stir Welding:

Friction stir welding (FSW) is a new, energy-efficient, appealing, and environmentally friendly solid-state welding technology that was invented in England in 1991 [4]. FSW appears to have several advantages over traditional fusion welding techniques, including the absence of costly consumables filler materials, good mechanical and metallurgical properties of the resulting joint, the absence of solidification cracks, no porosity, low distortion, and lower energy consumption [5]. Initially, this developing welding technology was utilized to join aluminum [4], but it has since been employed to join magnesium [6, titanium [7], copper [8, and ferrous alloys [9]. Combination of both parent material's good properties The challenges of connecting materials with significantly different characteristics using traditional fusion welding processes are well known.

FSW involves rotating and slowly inserting a cylindrical, shouldered tool with a profiled probe into the joint line between two butted pieces of sheet or plate material. The components are secured to stop the welding process from pulling the abutting joint faces apart. The materials to be connected and the wear-resistant welding equipment create frictional heat. The latter softens or melts as a result of the heat, making it possible to move the instrument along the joint line.

To create a weld between the two components, the plasticized material is moved from the tool probe's leading edge to its following edge and is forged by close contact with the tool shoulder. Increased productivity, particularly for thicker sections, the ability to weld almost all thermoplastics, the possibility of continuous welding, simple joint design, virtually flash-free welds, and the fact that it is an automated process, resulting in improved quality, and a decrease in weld failure are just a few of the potential benefits of FSW over existing fabrication welding techniques. The FSW technique currently has the drawbacks of only having been demonstrated to produce linear welds and not being commercially available to join polymers.

1.04 Principle of Operation:

The combining of different materials is critical since it is meant to produce a product with otherwise, the production of complex, brittle, intermetallic compounds can compromise weld quality, resulting in inferior welds. Similarly, due to compatibility concerns with physical properties of the materials as well as the creation of intermetallic compounds, it is not straightforward to directly link these materials utilizing solid-state joining methods. Friction stir welding uses significantly less energy than traditional welding processes, i.e. friction stir welding is better other welding process in FSW process, no cover gas or flux is utilized, therefore all of this advantage makes the process environmentally friendly.

The tool has two basic functions: (a) heating the work piece and (b) material movement to make the joint. Heat is generated through friction between the tool and the work piece, as well as plastic deformation of the work piece. A non-consumable cylindrical-shoulder tool with a threaded/unthreaded probe (pin) is rotated at a constant speed and inserted/plunged in-between the two separate work piece sheets or plates to be connected, then fed at a

consistent rate along the joint line depicted in figure 1.3. The tool primarily serves three purposes: (i) Material softening caused by heating of the work piece, (ii) material movement or plastic deformation to construct the joint, (iii) forging of the hot material behind the tool shoulder [4-5]. Due to friction between the rotating tool shoulder and pin and the work piece, as well as extreme plastic deformation of the work piece materials, heat is generated within the work piece and tool.

A non-consumable cylindrical-shoulder tool with a threaded/unthreaded probe (pin) is rotated at a constant speed and inserted/plunged between the two distinct work piece sheets or plates to be connected, then fed at a consistent rate along the joint line depicted in figure 1.3. The key functions of the tool are as follows: Material softening owing to work piece heating, material movement or plastic deformation to construct the junction, and hot material forging behind the tool shoulder [4-5]. Due to friction between the rotating tool shoulder and pin and the work piece, as well as high plastic deformation of the work piece materials, heat is generated within the work piece and tool. The primary function of the non-consumable spinning tool pin is to agitate the plasticized metal and transport it behind it in order to achieve a sound (or defect-free) connection [10].

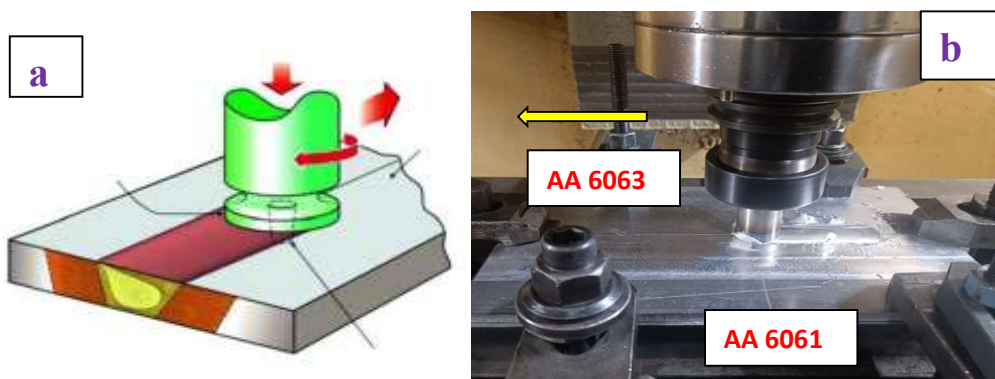


Figure 1.3: (a) FSW processing diagram Ref. <http://katjakovanen.com/Slavic-force-and-friction-experiments-for-kids/>. [17] (b) my own FSW experiment.

1.05 Advantages or Benefits of FSW

The following list of key advantages of friction stir welding for metallurgy, energy, and the environment is taken from [5, 11, 12].

❖ Metallurgical Advantage:

- Excellent mechanical and metallurgical qualities in the joint region;
- solid state joining technique;
- little distortion.
- Fine microstructure: After the grain is refined, fine equiaxed grain is produced
- Lack of porosity, solidification cracking, and hot cracking.
- Stress residue is minimal.
- No alloying elements were lost.
- Good repeatability and dimensional stability.
- Various materials and alloys can be welded together.

❖ Energy Advantage:

Improved materials-use (e.g., joining different thickness) allows reduction in weight and reduced fuel use in applications such as ships, cars, and light aircraft.

❖ Environmental Advantage:

There is no need for pricey consumables like filler, fluxes, and shielding gas.

No need to clean the surface.

Remove grinding byproducts.

No hazardous emissions.

1.06 There are certain disadvantage of FSW also and these are:

- When a tool is withdrawn, a hole remains.
- Long, tunnel-like flaws are caused by insufficient weld temperature and weld material's inability to accept significant deformation.
- To hold the plates together, strong down pressures and heavy-duty clamping are needed.
- Expensive Experiment Process.

1.07 Distinct Regions of Weld Zones

According to figure 1.4, the FSW weld zones are separated into four distinct regions [13,16].

Weld nugget: The tool pin-previously-occupied zone is referred to as the stir zone in the middle region of the weld, which is totally recrystallized and occupies fine equiaxed grains.

Thermo Mechanically Affected zone (TMAZ): There is typically a clear border between the recrystallized zone (weld nugget) and the deformed zones of the TMAZ in this area where the material has been plastically deformed by the FSW tool and some degree by the heat from the process.

Heat-Affected Zone (HAZ): The heat of welding causes changes in the microstructure and material properties in this area, although plastic deformation does not.

Unaffected Material or Base Metal: The structure or material qualities of the material are unaltered, but it may undergo a heat cycle because of the weld.

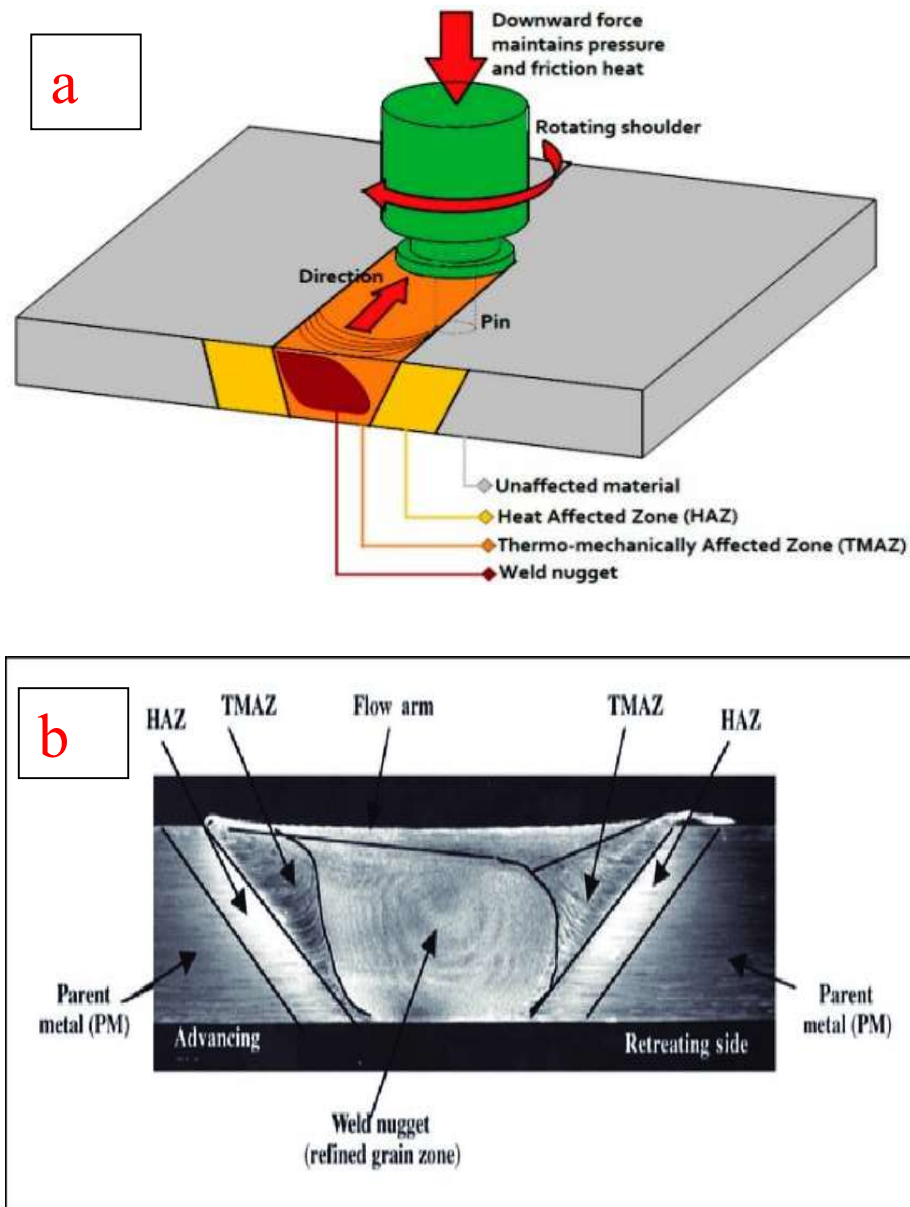


Figure 1.4: a) Schematic Diagram of FSW welding b) Different regions of Friction Stir Welded Zones Ref. <http://katjakovanen.com/Slavic-force-and-friction-experiments-for-kids/>. [17]

1.08 Welding Parameters and Their Role in Welding:

There are mainly three factors responsible for sound weld joint as shown in Figure 1.5.

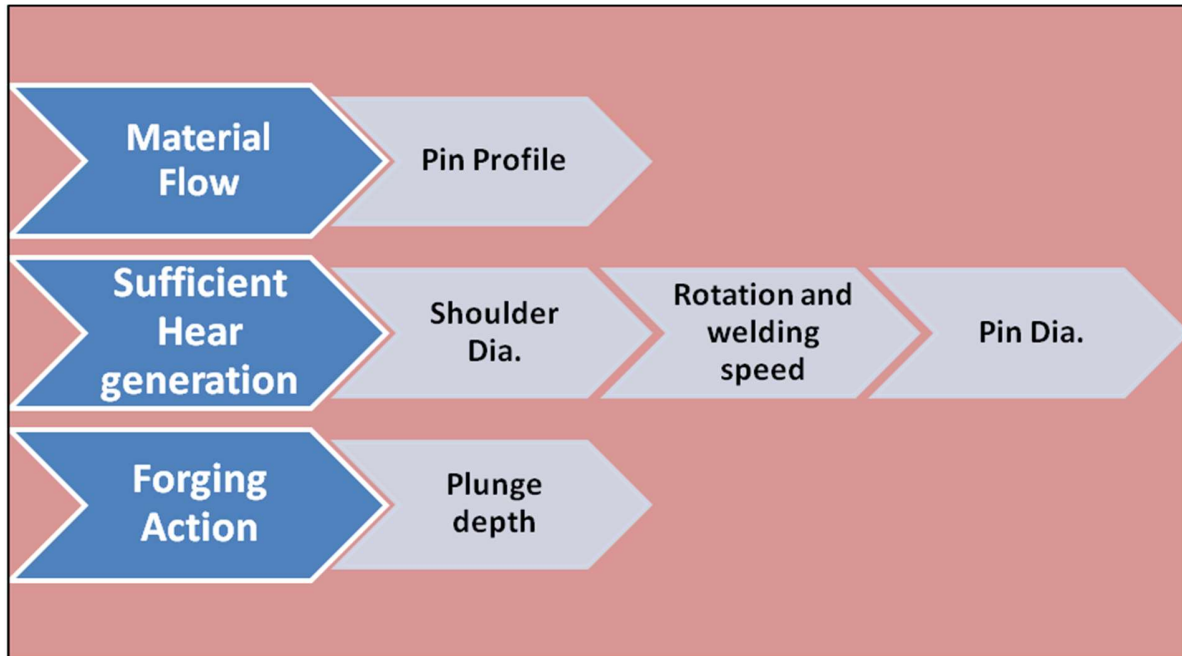


Figure 1.5: Factor responsible for a defect free joint

❖ Heat generation:

The friction between the rotating tool's shoulder and pin and the work piece, as well as the material's severe plastic deformation, cause heat to be generated inside the work piece and tool during FSW. Heat generation is influenced by the welding settings, weld tool form, thermal conductivities of the work piece materials, and backing anvil. The welding factors that affect heat generation include rotation and welding speeds, shoulder diameter, and plunge depth. Hot welds are often made with high rpm and low travel rates, whereas cold welds are frequently made with low rpm and high travel speeds. For a weld to be defect-free, sufficient heat generation is necessary.

In the stir zone, cold material may show voids or other faults, and in severe circumstances, the tool may break. On the opposite end of the spectrum, an excessive amount of heat input could be harmful to the weld's final qualities [12,14].

Most heat is produced by friction between the tool shoulder and the workpiece, but some heat is also produced by friction or plastic deformation between the pin tool and the workpiece, depending on whether slide or stick conditions are present at the interface. According to estimates, the heat input from deformational heating around the pin tool ranges from 2% to 15%.

❖ **Material Flow:**

The material around the pin is softened by the localized heating, and the combination of tool rotation and translation causes material to travel from the front to the back of the pin. However, the FSW tool profiles, FSW tool dimensions, and FSW process parameters have the greatest impact on the material flow behaviors.

A part of the metal is then swept by the mechanical working component of the process after the amount of metal heated is regulated by weld parameters in conjunction with the design and composition of the pin tool [15].

Tool Rotation speed:

The rate at which a tool rotates is referred to as its speed. This welding setting is essential for obtaining a junction without any flaws. When welding, the tool's rotational speed determines how much heat will be produced. Heat input will often rise if rotation speed is raised or traverse speed is decreased and vice versa. When the rotation speed is high, the material that has been stirred in the FSW zone is released, which causes a void to form in the upper surface. However, when the

rotation speed is low, proper mixing does not occur because the tool pin is not doing its job of stirring.

❖ **Welding or Traverse speed:**

Welding speed is the rate at which the tool moves along the joint line while welding. A significant factor in the productivity of the welded joints is welding speed. Due to insufficient consolidation during forging of the welded materials, voids are produced when the tool travels at higher speeds because heat output is reduced.

❖ **Tool Design and its role in welding:**

The tool's design plays a key role in productivity growth since it influences both the quality of the weld or joint strength that results from it and the fastest welding speed. Shoulder and pin make up the majority of a tool's design. The majority of heat produced during welding is caused by friction between the shoulder and the work piece when the shoulder is inserted within the work piece. This heat assists in softening the material, and once it has done so, tool pins are essential for welding. The non-consumable spinning tool pin's main job is to move the plasticized metal behind it and stir it in order to create a strong joint.

Pin profile is essential for controlling material flow, which in turn controls how quickly the FSW process welds [16]. The pin typically has flat, threaded, frustum tapered, and cylindrical plain surfaces. Square and triangular pin profiles with flat faces are linked to eccentricity. Incompressible material can move around the pin profile due to this eccentricity.

❖ **Welding Forces:**

The forces that are exerted on the tool during welding are listed below [16]:

- (i) **Downward force:** To keep the tool at or below the material surface, a downward force is necessary. When the tool is inserted into the material or, more specifically, when the shoulder contacts the work piece, this force increases.
- (ii) **Traverse force:** The traverse force is positive in the welding direction and acts parallel to tool motion. Given that this force results from the material's resistance to the tool's motion
- (iii) **Lateral force:** The lateral force is defined here as positive towards the weld's advancing side and may act perpendicular to the tool traverse direction.
- (iv) **Torque:** The amount of torque needed to spin the tool will depend on the downward force, the coefficient of friction (sliding friction), and/or the strength of the material's flow in the vicinity (sticking friction).

❖ **Plunge Depth:**

A vital factor in guaranteeing weld quality is plunge depth. In order to achieve sufficient forging of the material at the tool's back [18], the plunge depth is defined as the distance between the lowest point of the shoulder and the weld plate. This is depicted in figure 1.7.

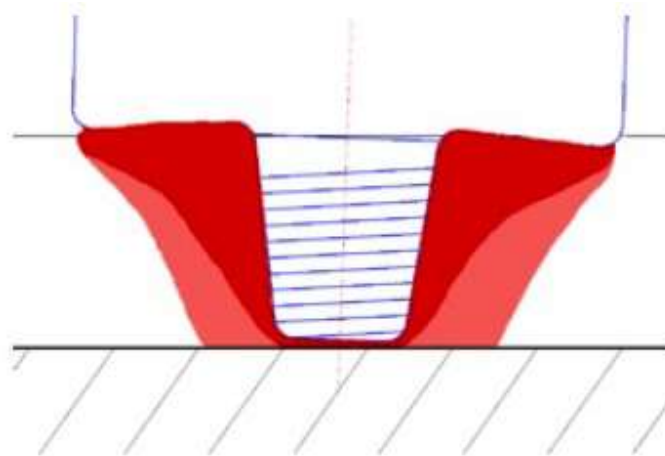


Figure 1.6: Schematic Plunge Depth of FSW Welding Ref.<http://katjakovanen.com/Slavic-force-and-friction-experiments-for-kids/>. [17]

❖ Tool Tilt:

It has been demonstrated that tilting the tool by 0–2 degrees so that the rear of the tool shoulder is lower than the front will help the forging process [18].

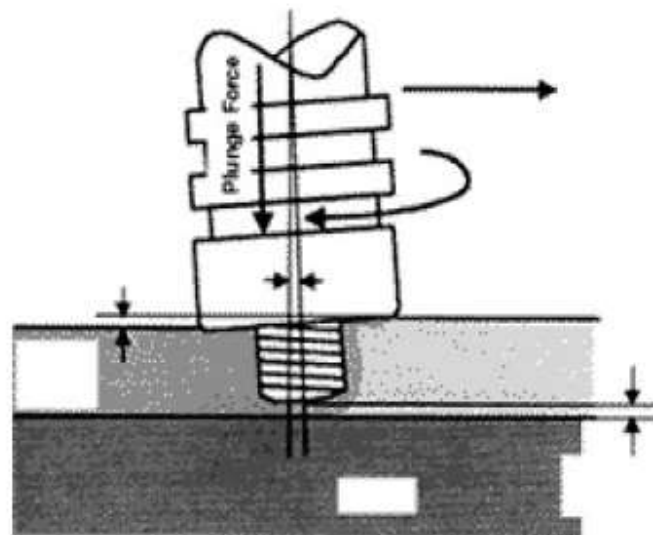


Figure 1.7: Schematic FSW Tool Tilt Angle Ref. <http://katjakovanen.com/Slavic-force-and-friction-experiments-for-kids/>. [17]

❖ Dwell:

This is the period when the tool is just continuously rotating into the material of the work piece to produce enough heat to soften the material before it is moved in the direction of welding.

1.09 Application:

Due to their differing properties and material incompatibility, connecting different alloys of dissimilar metals with thermoplastic and composites is a difficult task. The fabrication process known as friction stir welding (FSW) welds materials below their melting point and has become a cutting-edge approach for joining metals that are like one another but not the same. As the produced temperature is below the melting point of the base material, FSW has many advantages over conventional welding techniques. This enables the base materials to achieve an elastic phase with the least amount of distortion, residual stresses, and flaws. FSW has numerous uses in the transportation, aviation, maritime, rail, and aerospace industries because of these characteristics.

Due to its high weld quality and geometry accuracy, it is used in the aerospace sector to fabricate structures like airframes, thin alloy skins, fuel tanks; in the automotive industry to manufacture lightweight vehicles; and in the railway business to construct heavy-duty tanks, railway wagons, and coaches.

Aluminium alloys are widely employed in a wide range of simple to complicated applications, including the construction of aircraft bodies. There are situations where different series of aluminium alloys need to be linked because of the variety of service circumstances. The 3xxx,

5xxx and 6xxx family of non-precipitation hardenable aluminum alloys are the most widely utilized in aerospace applications.

The 2xxx, 6xxx, and 7xxx series of Al alloys are a few of the precipitation-hardenable series. While the 7xxx series exhibits exceptional corrosion resistance and good mechanical qualities at low temperatures, the 2xxx series has the advantage of having outstanding mechanical properties at high temperatures. When considering how well these materials perform in service and under what conditions they actually perform in service, it is crucial to identify the best joining method and process parameters to use. Alloys made of aluminium are lighter while yet being strong and flexible. Because of this, the material is a better choice to work in a variety of working environments.

Aluminium alloys AA6061 and AA6063 are frequently used in the shipbuilding, aircraft, and automotive industries. Fusion welding of different aluminium alloys is highly difficult, partly because the constituent elements form low melting eutectics that cause weld solidification cracking. Aluminium alloys are quite sensitive to the metal compositions of the welds when it comes to hot cracking. As a result, since solid state joining does not involve melting, it is more appropriate for welding aluminium alloys. This technology can therefore be used to prevent flaws including weld solidification cracking, porosity, segregation, liquid cracking on heat-affected zones, and brittle intermetallic formation. In FS welding procedures, tool shape is crucial for achieving the desired mechanical and metallurgical qualities.

CHAPTER -2

LITERATURE REVIEW

Prior to the development of FSW in 1991, some aluminum alloys were challenging to weld using traditional fusion welding due to poor fatigue and fracture strength of these alloys as a result of poor solidification microstructure and porosity in the fusion zone. Due to their low weld ability, these alloys have a limited range of applications, and fusion welding is not a desirable joining method for aluminum alloys. In 1991 in Cambridge, England, The Welding Institute developed a novel joining method known as Friction Stir Welding to address this issue. W. H. Thomas and others were listed as the inventors in US Patent Application No. 5,460,317 for FSW, which was given to TWI [1, 7].

The FSW technique has quickly advanced in aluminum alloys and been successfully applied in industrial settings, which has inspired its use in other metals like magnesium (Mg), copper (Cu), titanium (Ti), ferrous alloys, and even thermoplastics. This joining procedure was initially applied to alloys of aluminum. Welding high temperature materials like steel and titanium is a challenge since efficient welding tool materials are required [1–9].

A new, environmentally friendly, and energy-efficient solid state joining method is friction stir welding. Solid state joining is when welding takes place below the melting point. Typically, temperatures approach 80% of the melting point because of this solid state nature, which results in a high-quality weld. This property completely eliminates solidification flaws and significantly lessens the negative impacts of excessive heat input, such as distortion. Environmentally friendly, friction stir welding is also very effective, emits no fumes, and requires no filler material [8].

Peel et al. [9] employed just one type of pin profile (cylindrical threaded) for welding in FSW of dissimilar aluminium alloys, and this paper helps to attain the optimisation parameters and

illustrates the viability of welding two dissimilar aluminium alloys (AA 5083-AA 6082). They discovered minimum hardness is where the tensile test fractured, which is the heat affected Zone (HAZ), and minimum hardness is caused by precipitate coarsening from excessive ageing.

Elangovan et al. [10] employed five types of various pin profiles, including straight cylindrical, cylindrical taper, cylindrical threaded, triangular, and square, on AA 6061 and examined the effects of all five pin profiles.

H. Fuji et al.'s inquiry [11] into the impact of tool form on the mechanical characteristics and microstructure of aluminium alloys. They welded three different types of aluminium alloys, 1050-H24, 6061-T6, and 5083-O, using three different pin profiles: straight cylindrical, threaded cylindrical, and triangular prism form probes.

R. PALANIVEL et al. [12] investigated the impact on mechanical and metallurgical properties of dissimilar AA6051- AA5083H111 by using five different tool pin profiles: straight cylindrical, threaded cylindrical, square, tapered square, and tapered octagon.

Objective and Scope of Present Work

According to the literature review, friction stir welding (FSW) is best suited for aluminium alloys, and the weldments created by this method depend on the tool's rotational speed, profile, and other factors. The interchangeable molecular atoms in the metal during friction stir processing led to good characteristics at 2000 rpm and poor strength at 2500 rpm, according to the mechanical and microstructural analysis. The purpose of the study is to discuss the impacts of welding parameters on FSW aluminium weldments, such as tool rotational speed, and to identify the ideal circumstances for producing weldments that are strong and free of flaws.

The tool rotation speeds used in this investigation are **1000, 1500, 2000, and 2500 rpm**. Four samples of the dissimilar aluminium alloy AA6061 & AA6063 having 6 mm thickness underwent testing at a **60mm/min** travel speed. A better knowledge of the mechanical characteristics and microstructure at lower speeds to higher at constant travel speeds in dissimilar FSW AA6061 & AA 6063 weldments would result from this work.

At a tool rotational speed of 2000 rpm, a better weld with good tensile strength and fine grain microstructure was produced, according to microstructural analysis and mechanical testing methods on sample weldments.

Due to their excellent strength to weight ratio and strong corrosion resistance, aluminum alloys find extensive use in aircraft, transportation, shipbuilding, and marine industries. In particular, it was thought that the heat-treatable 6xxx series, particularly 6061-6063, was more suited for maritime frames, pipelines, and airplanes. However, there were several difficulties encountered when such an alloy was welded using traditional fusion welding techniques, including low weld ability, solidification cracking, and distraction stress.

The use of the friction stir welding (FSW) method is the most practical solution to this problem. The material becomes soft during this procedure as a result of the application of intense localized heat caused by the tool's stirring action. The revolving tool causes plastic deformation and solid-state joining when it contacts the work piece surface and plunges into the adjacent base material. Additionally, there is significant wear caused by the aluminum alloys coming into touch with the stiffer particles.

When stiff particles such as oxides (Al_2O_3 , TiO_2 , etc.) and carbides (SiC , TiC , etc.) or their mixture were introduced to the aluminum alloy base matrix, this issue was resolved. When compared to unreinforced alloy, it aids in improving the mechanical and tribological properties of aluminum alloy.

CHAPTER -3

EQUIPMENT'S USED.

3.1 Lathe Machine:

A type of machine tool called a lathe, as depicted in figure 3.1, rotates the work piece about its axis while performing a number of operations, such as cutting, knurling, drilling, or deforming the work piece with tools to create an object with symmetry about the axis of rotation. I intended to use the cylindrical shoulder tools I have made.



Figure 3.1: Lathe M/cused for making FSW cylindrical shoulder Tools.

3.2 Cut Saw:

As seen in figure 3.1(B), a saw is a device that slices through soft materials using a hard blade or wire with a serrated edge. We cut the needed size of work piece from a huge sheet using an electricity-powered saw.

3.3 Milling Machine:

As seen in figure 3.2(A), a milling machine is a type of machine tool used to work with solid materials. A spinning cutting tool known as a milling cutter is used by the milling machine to remove metal. Boring, slotting, drilling, and circular milling and dividing can all be done with milling machines. I made tool pin profiles with the aid of indexing using this machine for sample facing. Additionally, this machine may be used to flute taps and reamers as well as cut keyways, racks, and gears.



Figure 3.2: (a) Milling Machine & (b) Belt Emery

3.4 Belt emery:

A mechanical grinding device called a belt emery is used to remove extra scrap that results from milling work piece samples. As seen in picture 3.2 (b), this machine consists of an abrasive belt.

3.5 Vertical CNC Milling with Friction Stir Welding (FSW) Tools:

As illustrated in figure 3.3, this machine offers rotation speeds of 20 to 5000 rpm and traverse speeds of 0.1 to 2000 mm/min with axial forces of up to 100 KN. To provide the ideal conditions for welding, we may adjust the three axis moments in this machine.

The experimental study involves butting together 6 mm thick plates made of the aluminium alloys AA6061 and AA6063. As seen in figure 3.4, the welding procedure is carried out on a vertical milling machine (Make STM, 10hp, 5000rpm). Tool arbour will hold the tool. The entire FSW welding experimental set up is depicted in figure, along with special welding fixtures and jigs that are made to accommodate plates measuring 150 mm X60 mmX 6 mm for both graded AA Alloys (AA6061 & AA6063).



Figure 3.3: Milling Machine with FSW Tool Mounted in Tool Arbor

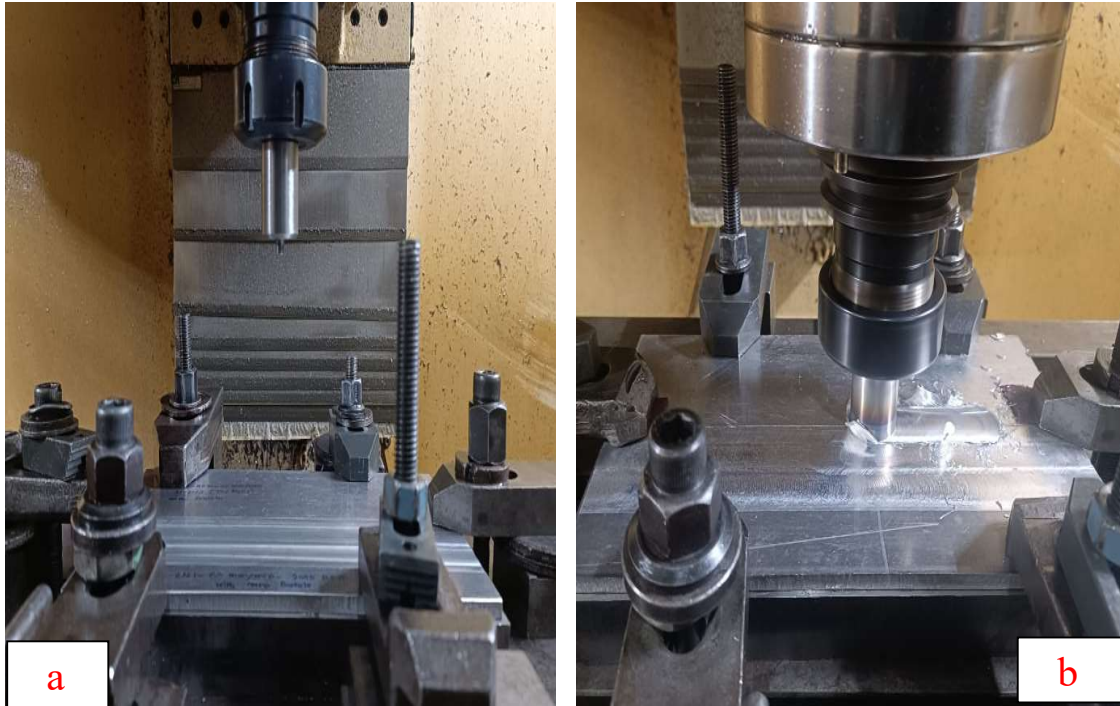


Figure 3.4: (a) Two type of dissimilar plate (AA 6061 & AA6063) is clamped in Milling M/c (b) FSW Welding in Milling Machine by FSW Tool Mounted in Tool Arbor

3.6 Cutting Machine:

As shown in figure 3.5(a), Secotom (precision cutting) carries out accurate and quick deformation-free cutting for various types of materials including metals, ceramics, biomaterials, and minerals. I utilized this machine to cut a transverse piece out of a welded sample that was 50 mm by 10 mm by 6 mm in size.

3.7 Grinding machine:

SiC grinding papers (180-500 Grit) are needed, and they must be turned on a wheel at a speed of 300–800 rpm while the sample is pressed face down, cooled, and cleaned with water as illustrated in figure 3.5(b). These are also referred to as fixed abrasives since the little SiC particles are bound to the grinding paper. These particles gently remove chips from the specimen surface as they are rotated.

3.8 Polishing Machine:

As illustrated in figure 3.6, this polishing equipment is like a grinding machine except that the abrasive particles are free and water cooling is not used.⁸ The employed diamond suspension has particles with a diameter of 1 to 9 μm . This is an automatic polishing device that automatically supplies the necessary amount of diamond suspension particles.



Figure 3.5: (a) Cutting Machine (b) Grinding machine.

3.9 Optical Microscope:

The optical microscope, commonly known as the "light microscope," is a type of microscope that enlarges images of three microscopic samples using a series of lenses and visible light. As seen in figure 3.6(b), I used a Leica hot stage automated upright microscope.



Figure 3.6: (a) Polishing machine (b) Optical Microscope

3.10 Vickers Micro hardness:

When "macro" hardness tests are incorrect, it is possible to assess the microhardness of metals, ceramics, and composite materials. Static indentation with loads less than 1 kgf is frequently referred to as a "micro hardness test". Figure 3.7 (a) depicts the Dura Scan 20 Emco- Test Vickers hardness using an indenter with a diamond pyramid form.

3.11 Tensile Machine:

The INSTRON Load Frame, which is visible in Figure 3.7(b) and features a hydraulic operating mechanism, is used for tensile testing.

3.12 Corrosion Tester Machine:

Corrosion is a process that causes metal to deteriorate or degrade. The development of rust on steel is the most typical example of corrosion. The majority of corrosion processes is electrochemical in nature and includes at least two surface reactions on the corroding metal. The corrosion test is performed by AUTOLAB Corrosion Tester m/c which is shown in figure 3.8.



Figure 3.7: (a) Vickers Micro hardness Tester (b) Sample fitted with extensometer in INSTRON m/c

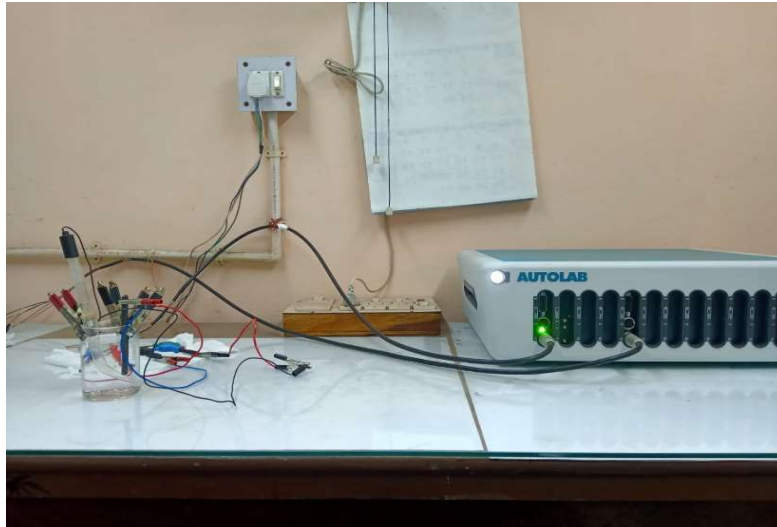


Figure 3.8. AUTOLAB Corrosion Tester m/c

3.13 Scanning Electron Microscopy (SEM):

An energy dispersive X-ray (EDX) for composition analysis was added to a scanning electron microscope (SEM) (Model HITACHI SU3800) to analyze the microstructure of friction stir welded different Al alloys. A 20 KV accelerated voltage has been used to run the SEM. The scanning electron microscope's photographic view is depicted in Figure 3.9. The microstructures have been studied using both back scattered electron (BSE) and secondary electron (SE) imaging techniques. For the chemical characterization of the material, EDX technique has been employed. In the following chapter, the figures are presented.

3.12 Fractography

After the tensile test, transverse portions were sawed off the gauge component. SEM images of sample fracture surfaces were captured at various magnifications, including 500X, 1000X, 2500X, and 5000X.



Figure 3.9. HITACHI SU3800 SEM

CHAPTER -4

EXPERIMENTAL PROCEDURES

Experimental Procedure

This chapter describes the experiment that was conducted for the current inquiry. It involves the choice of materials, the creation of FSW Tools, FSW welding at various RPMs, tensile testing, and fractography observation.

The Experiment is given below:

- ❖ Material Selection and Chemical Analysis of the Materials.
- ❖ Tools preparation of FSW welding.
- ❖ Sample preparation for microstructure analysis, hardness and tensile testing and grain size determination before FSW Welding.
- ❖ FSW Welding is carried out dissimilar aluminum grade (Al 6061 & Al6063) at different RPM.
- ❖ Sample preparation of Tensile Testing of FSW Welded Al Alloys.
- ❖ SEM Fractography after testing.
- ❖ Micro Hardness Testing.
- ❖ Corrosion Testing of AA 6061 and AA 6063 & Welded Sample at three different solution

4.2 Material Selection and Chemical Analysis along with Mechanical Properties:

4.1.1 Work piece materials:

Aluminum alloy AA 6061-T6 is a precipitation-hardened aluminum alloy that is mostly composed of magnesium and silicon. It has strong mechanical qualities, is weld able, and is frequently extruded. It is one of the most prevalent general-purpose aluminum alloys.

It has Excellent joining qualities and coating acceptability. Combines moderate strength with decent work skills.

Aluminum alloy AA 6063-T6 contains magnesium and silicon as alloying components. The most prevalent alloy for aluminum extrusion is 6063. It is used for visible architectural applications such as window frames, door frames, roofs, and sign frames because it permits complex designs to be created with very smooth surfaces suitable for anodizing.

It is typically utilized in complex extrusions. It has a good surface polish, great corrosion resistance, is easily welded, and can be anodized.

4.1.2 Work piece Dimensions

By using a power saw and NC milling to face mill the appropriate size of (150 mm x 50 mm) from two different aluminum plates (AA 6061 and AA 6063) of thickness 6mm, excess scraps from the work piece were removed.

Chemical composition of the material has been studied by using an Optical Emission Spectrometer (Model No MA 3460 Make Thermo Electron Switzerland).

Mechanical Testing of material has been studied by using INSTRON Universal Testing machine (Model No INSTRON 8801).

Table4.1 : Chemical Composition and Mechanical Properties of Al 6061

Element	Al	Mg	Si	Cu	Cr
Wt %	95.86	0.84	0.4	0.15	0.04

Tensile Strength	Yield Strength	Elongation	Hardness
310 MPa	276 MPa	Upto 15%	95 VHN

Table4.2 : Chemical Composition and Mechanical Properties of Al 6063

Element	Al	Mg	Si	Cu	Cr
Wt %	99.35	0.6	0.05	0.01	0.02

Tensile Strength	Yield Strength	Elongation	Hardness
180 MPa	214 MPa	Upto 33%	51HV

4.2 Tools Design and Tool Pin Profile

Because of its high hardness, high strength, toughness, good oxidation resistance, low thermal conductivity, ease of manufacturing, low cost, and simple availability in the market, H13 tool steel is preferred over a variety of other tool materials, including high speed steel, tool steel, high carbon, high chromium steel (HCHCr), carbide, and tungsten, among others, for fabrication of weld joints.

Pin profiles can be produced utilizing indexing on a lathe and NC milling machine, as shown in Figure 4.3. After manufacture, tools are oil hardened to a hardness of 48 to 52 HRC.

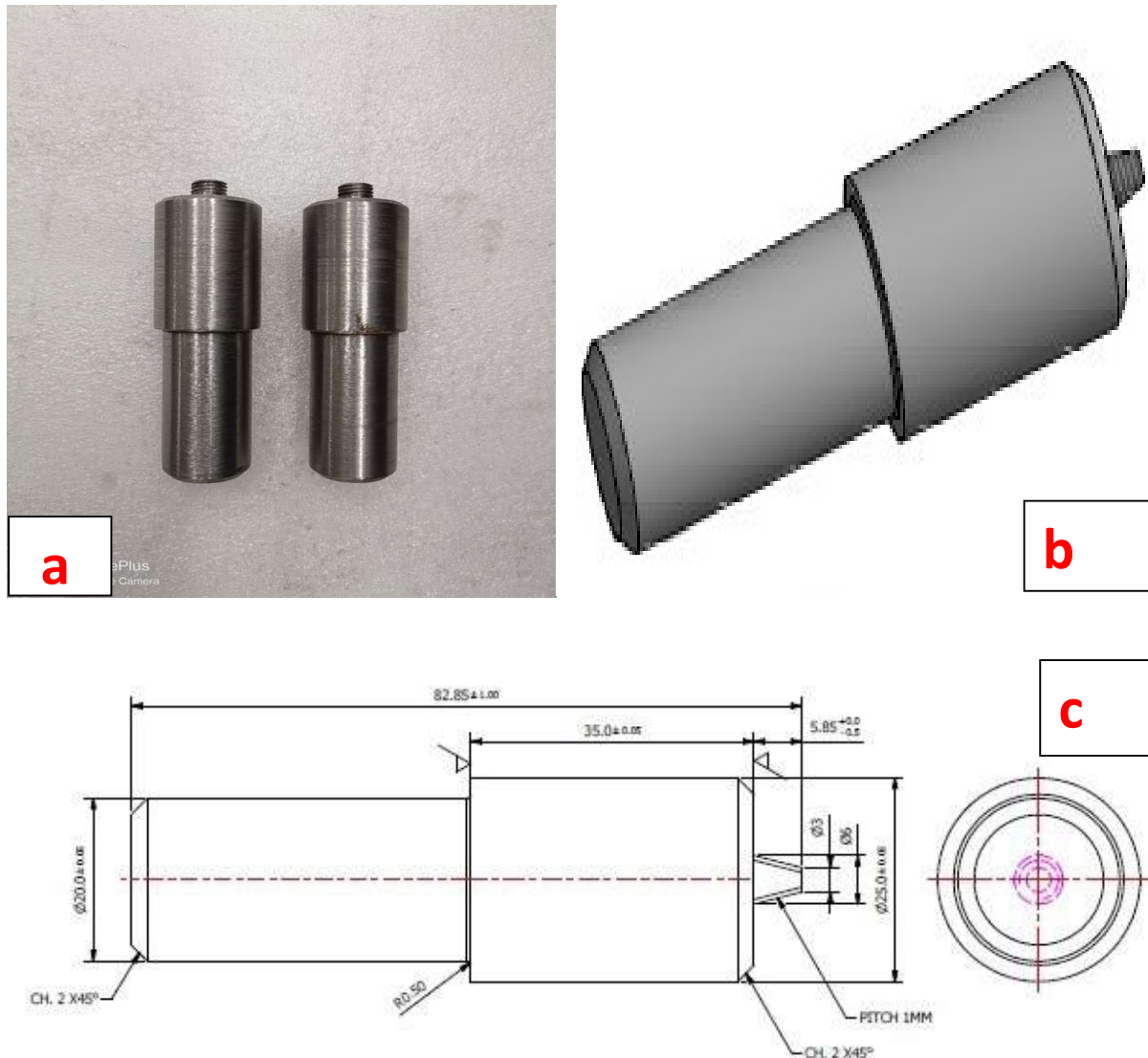


Figure 4.1(a) FSW Tools by made by H13 Steel with Threaded Pin Profile (b) 3D view of FSW Tool drawn in Solid Works software (C) 2D detail dimension of FSW Tools

Table 3 provides information on the dimensions of the tool and the welding process parameters. The tool has a shoulder diameter of 18 mm having pins with diameters of 6 mm each, circumscribed threaded pin with a right-hand pitch of 1.0 mm and a length of 5.85 mm.

Table 4.3. Optimized Welding Parameters

Pin Profile	RPM	Feed Rate mm/min	Shoulder Dia (mm)	Pin Dia (mm)	Pin length (mm)	Plunge Depth (mm)
Threaded	1000	60	18	6	5.85	0.5
	1500	60				
	2000	60				
	2500	60				

4.2 FSW Welding: CNC Vertical Milling machine is used to weld work piece sheet or plates by FSW Tool with threaded pin profile used for welding. This machine offers rotation speeds between 20 and 5000 rpm and traverse speeds between 0.1 and 2000 mm/min with axial forces up to 100 KN. Visual inspection and optical microscopy observations of each FSW joint are used to determine the optimal welding parameters in an effort to produce sound (defect-free) joints.



Figure 4.2: FSW welded Dissimilar Al alloys (AA 6061 & AA 6063) with RS and AS and Welding Direction.

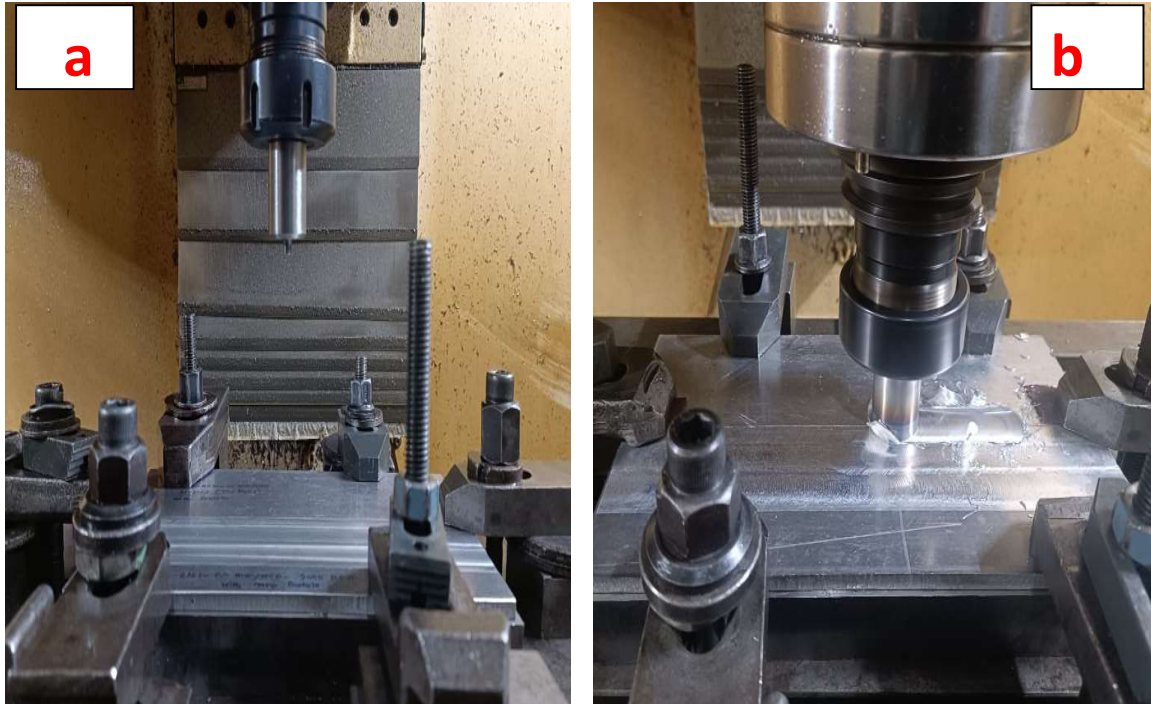


Figure 4.3: (a) Clamping of diff grade Plates for FSW Welding in Milling Machine by FSW Tool Mounted in Tool arbor (b) FSW Welding is running at diff tool rotation



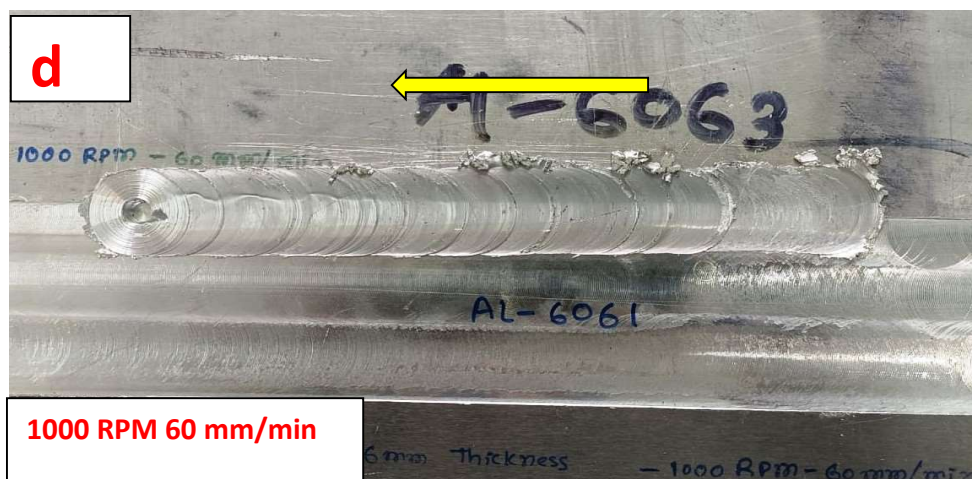
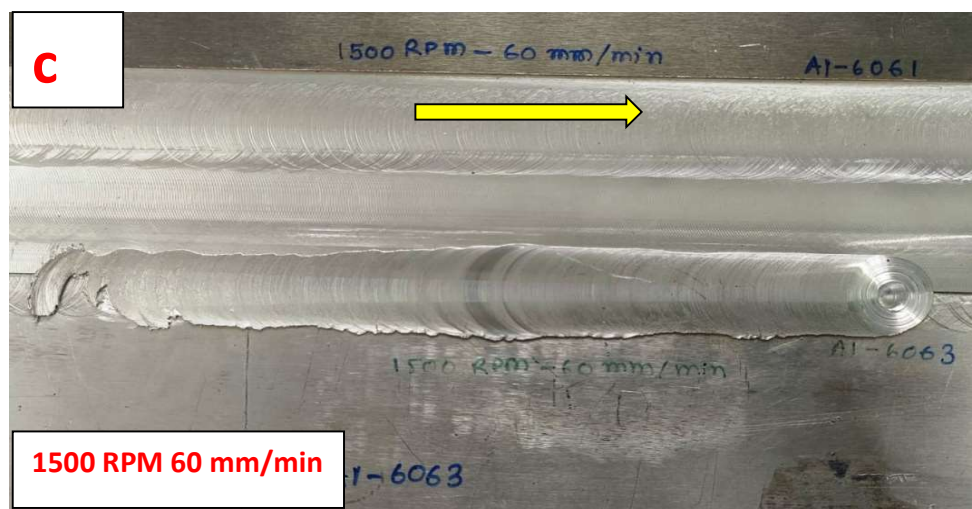
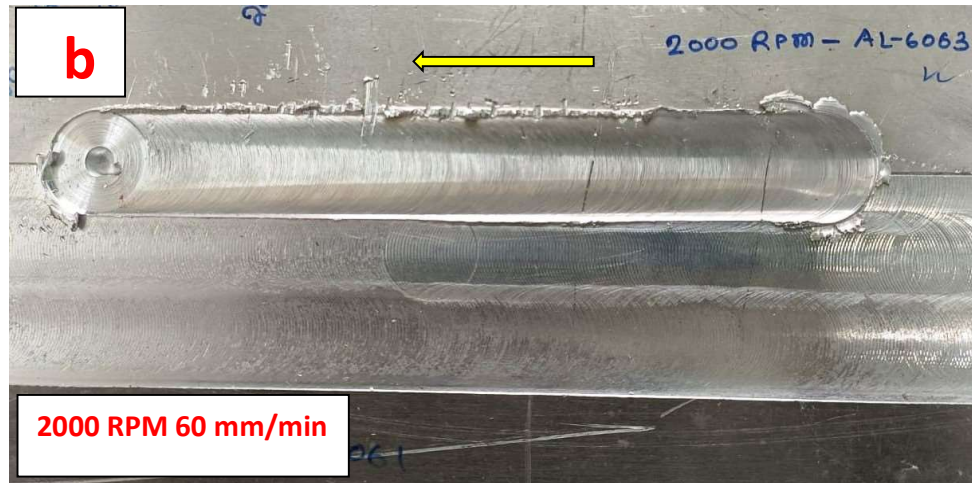


Figure 4.3: Dissimilar Al Alloys welding by FSW process with different RPM (a) 2500 RPM (b) 2000 RPM (c) 1500 RPM (d) 1000 RPM

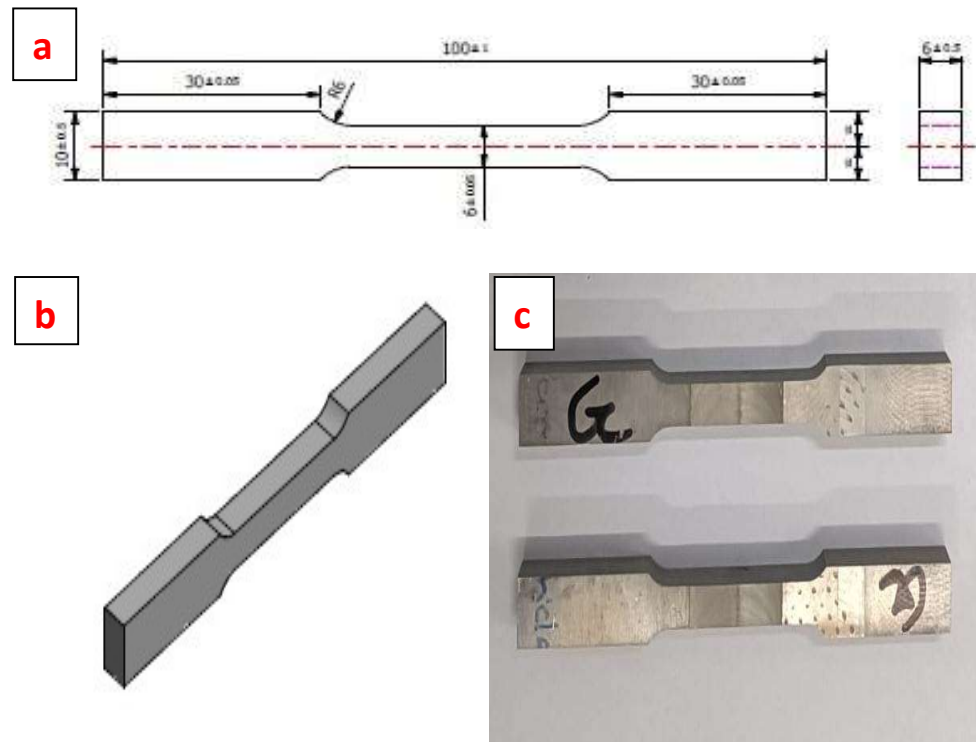


Figure 4.4: Tensile Specimen as per ASTM E8M standard (a) 2D detail Dimension (b) 3D View (C) original sample prepared after FSW welding followed by Wire Cut EDM

Tensile Testing: With the use of wire EDM, dog bone-shaped tensile test specimens are created, which are then prepared perpendicular to the welding direction and tested on an MTS machine with a strain rate of 0.001/sec.

Microstructure and SEM Analysis: To test the hardness and microstructure of the welded sample, a precision cutting machine (Secotom) with dimensions of 50 mm x 10 mm x 6 mm is used to cut the sample on the transverse section perpendicular to the welding direction.

The FSW specimens were electropolished for 15 to 25 seconds at 12 volts while being etched using Keller's reagent and 30% nitric acid in methanol. They were photographed using optical microscopy at a 5X magnification.

The transverse sections of the specimens were then optically imaged, and numerous zones were discovered, including the base material, the interface, the nugget or stir zone, the thermomechanical affected zone (TMAZ), and the heat impacted zone (HAZ). Additional microstructural characterization of the welded samples' various areas, including the nugget, (TMAZ), (HAZ), and base materials, is carried out using a scanning electron microscope and electron backscattered diffraction (SEM).

Micro hardness Test:

On a Micro Vickers Hardness Tester, a micro hardness test was conducted. Micro hardness testing is conducted using the indentation method. With the aid of a diamond pyramid, a permanent deformation was produced on the test sample's surface. The load necessary to cause a deformation of a specific dimension was used to compute the hardness of the test sample.

Vickers hardness tests were conducted using a 0.1 kg load that lasted for 10 seconds. Following the indentation, the horizontal and vertical diagonals of the diamond impression were measured using the scale of the eyepiece. The tester was calibrated to provide the micro hardness results immediately. The micro hardness was measured at distances ranging from 5 mm from the center to 35 mm.

Corrosion Test:Al has a higher CR than other materials because it contains an oxide layer that acts as protection. This study's main goal was to evaluate the weld area and the corrosion rates (Crs) of the alloys AA6061 and AA6063 in hostile conditions.

The corrosion test was created to find out how resistant the material was to corrosion in various environments, such as basic, saltwater, and acidic ones. The failure analysis of industrial and construction materials frequently uses this corrosion test. Corrosion can take many different forms,

including intergranular, stress, galvanic, fretting, uniform, pitting, erosion, and atmospheric corrosion. In laboratory submersion testing, the CR is quickly ascertained by lowering the error. These assays are easy to perform and allow for speedy specimen screening.

SI No	Solution	pH Value	Temp ° C	Submersion Time (Days/Hour)
1	3.5% HCL +H2O	3.12	30	12/288
2	3.5% H2SO4 +H2O	3.56		
3	Sea Water (3.5% NaCl)	7.58		

Figure 4.5: Corrosion Solution Tensile Specimen as per ASTM E8M standard

The submersion test adhered to the ASTM G3 standard. Three test mediums were utilised for the submersion test. One of the media was alkaline seawater, and the other two were acidic (3.5 wt percent HCl + H₂O and 3.5 wt percent H₂SO₄ + H₂O). The foundation materials (AA6061 and AA6063) and the weld area were used to build the test specimens, which had the dimensions 18 12 6 mm³. A digital pH metre was used to calculate the pH levels of the two acidic solutions, the seawater, and other materials utilised in the submersion test.

Table 4.5 displays the weight percentages of several corrosion test solutions, submersion time temperatures, and solution pH values.

The weight loss approach was used in the submersion test. Before being submerged in distilled water and dried by air, the specimens were polished and cleaned with acetone. Prior to the submersion test, the initial weight of each specimen was calculated. Glass beakers were used to

immerse the specimens from the AA6011 and AA6063 base materials, as well as the weld area, in HCl solution, H₂SO₄ solution, and seawater. The samples were stored for 12 days at 32 °C. The samples were removed from the immersion solution at the conclusion of the submersion test and allowed to fully dry (12 days later).

Using a digital scale, the test specimens' ultimate weights were determined. The weight loss of each specimen after 12 days was calculated using the difference between the initial weight of each specimen before the submersion test and the final weight of the same specimen after the submersion test.

CHAPTER -5

RESULTS AND DISCUSSION

5.0 Introduction

Different type of properties, such as tensile deformation, microhardness, and corrosion resistance of the AA6061 alloy base, AA6063 alloy base and dissimilar friction stir weld joint produced at different rotational speed has been discussed. Furthermore, the tensile properties of the base alloys and FSW weldments have been correlated with the microstructural features. Moreover, the change in the fractography at different conditions has been investigated. The variation of microhardness at different location near to FSW weld joint has been measured. Additionally, the corrosion resistance of the base alloys and FSW weldments has been thoroughly investigated.

5.1 Tunnel Defect:

The tunneling FSW fault is among the most serious varieties. When there is insufficient material flow around the tool pin, an irregular weld filling results, which causes the tunneling flaw. This type of defect is found at tool rotation of 1000 and 1500 rpm; however, the occurrence of such defects is found to be absent at tool rotation of 2000 and 2500 rpm.

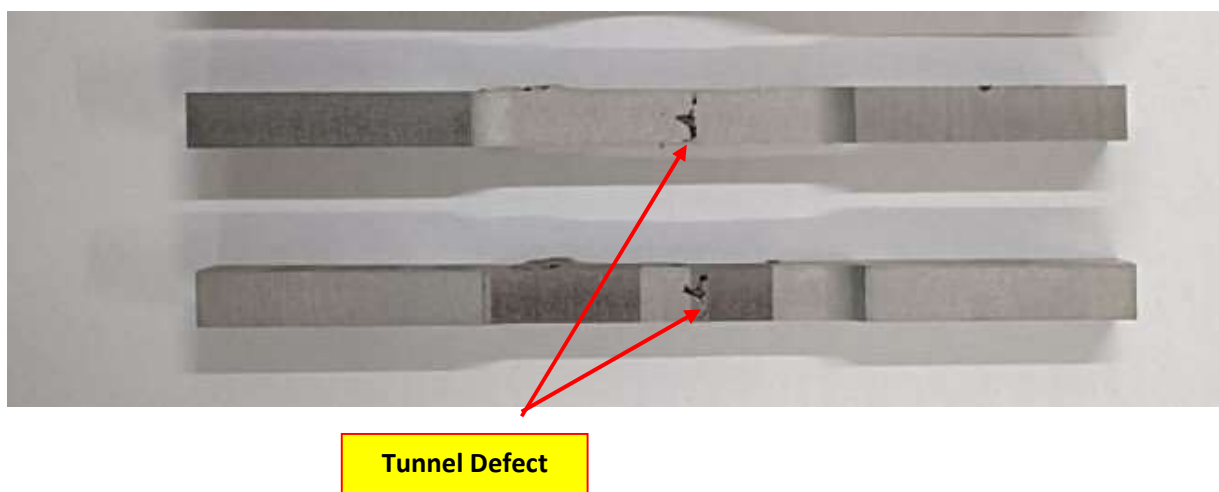


Figure 5.1: Tunnel defect in FSW welding at tool rotation 1000 rpm, 1500 rpm and 2500 rpm

5.2 Mechanical Testing:

The tensile deformation curves at room temperature of the base AA6061 and AA6063 alloys, as well as FSW weld joints produced at different rotational speed of 1000, 1500, 2000 and 2500 rpm, as depicted in Figure 5.1, has shown completely different nature of tensile deformation behavior. The base AA6061 alloy has revealed a significantly large uniform elongation region, whereas the uniform elongation region is found to be limited in the base AA6063 alloy and the weldments except produced at the rotational speed of 2000 rpm. The uniform elongation region in the weldments produced after FSW at 2000 rpm appears to be better than the base AA6063 alloy, but inferior than the base AA6061 alloy. Moreover, the tensile deformation curves and uniform elongation regions are found to be a function of rotation speed of friction stir welding process. With the increase in the rotational speed of the FSW process, the tensile deformation curves and uniform elongation region appears to be improved. The tensile deformation curves and uniform elongation regions are found to be better than the base AA6063 alloy in the weldments produced at the rotational speed of 2000 and 2500 rpm. However, the tensile deformation curve is found to be best in the weldment among different conditions.

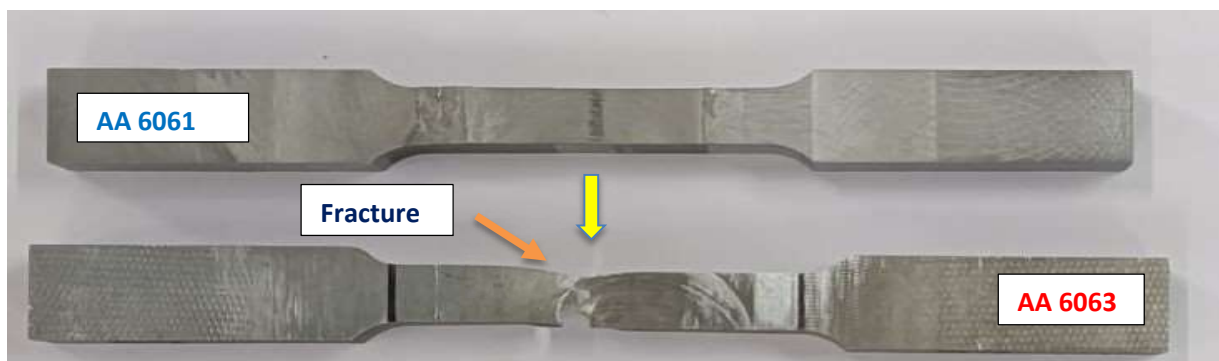


Figure 5.2: FSW Fracture Specimen after tensile testing

The key independent factors, such as the welding speed, the tool rotating speed, the vertical pressure on the tool, the tool tilt angle, and the tool design etc. control the FSW process. These factors influence the pace of heat generation, the temperature field, the rate of cooling, the x-direction force, the torque, and the power. Consequently, the tensile properties, i.e., yield strength (YS); ultimate tensile strength (UTS) and total elongation are expected to be different in the weldments fabricated at different rotational speeds. The tensile parameters, i.e., yield strength, ultimate tensile strength, and total elongation of the base alloys and weld joints fabricated at rotational speed of 1000, 1500, 2000, and 2500 rpm, and a welding speed of 60 mm/min, are shown in Table 5.1 and Figure 5.2.

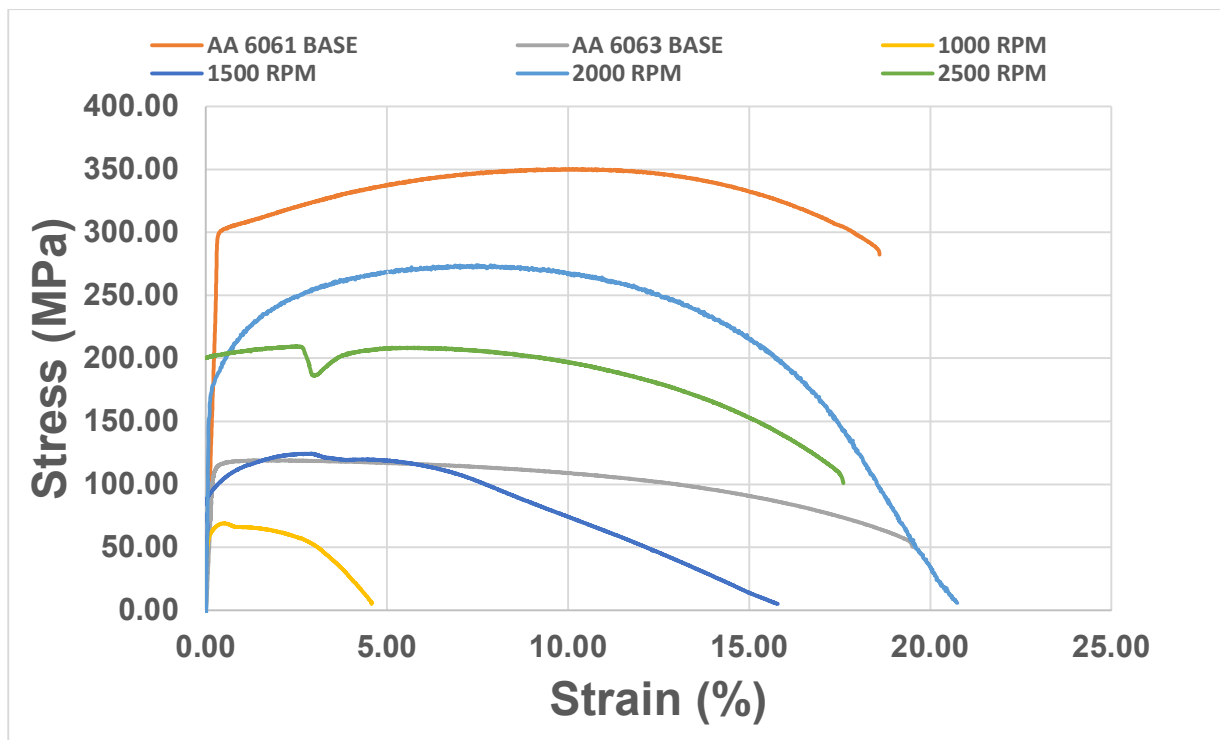
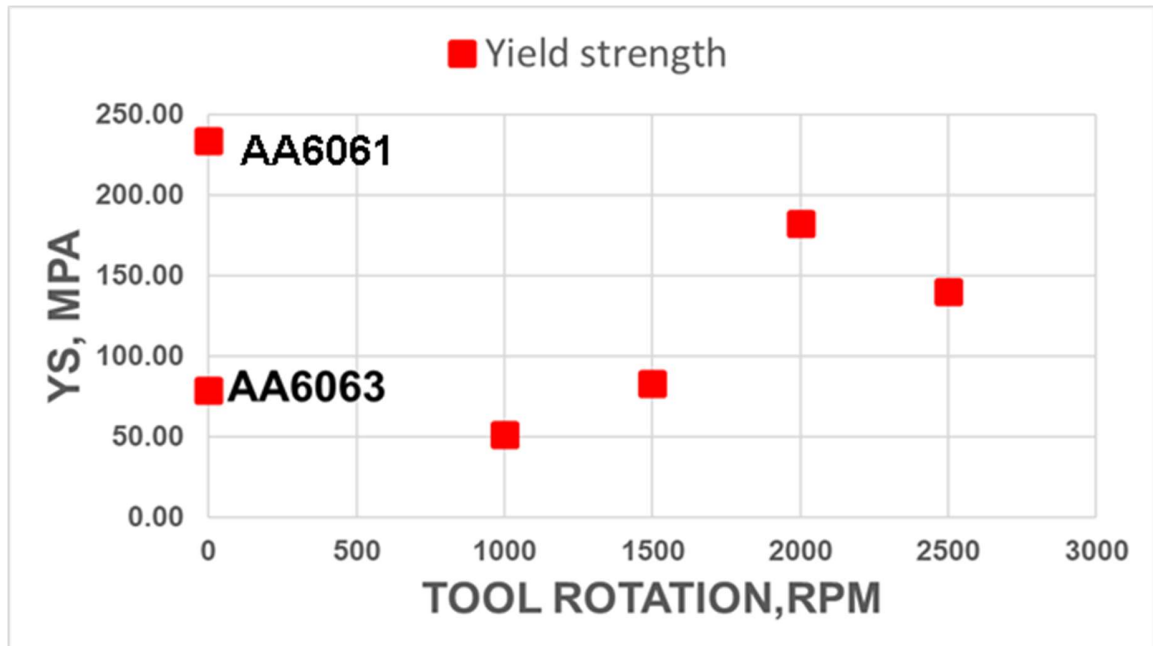


Figure 5.3: Room temperature tensile deformation curves at different conditions

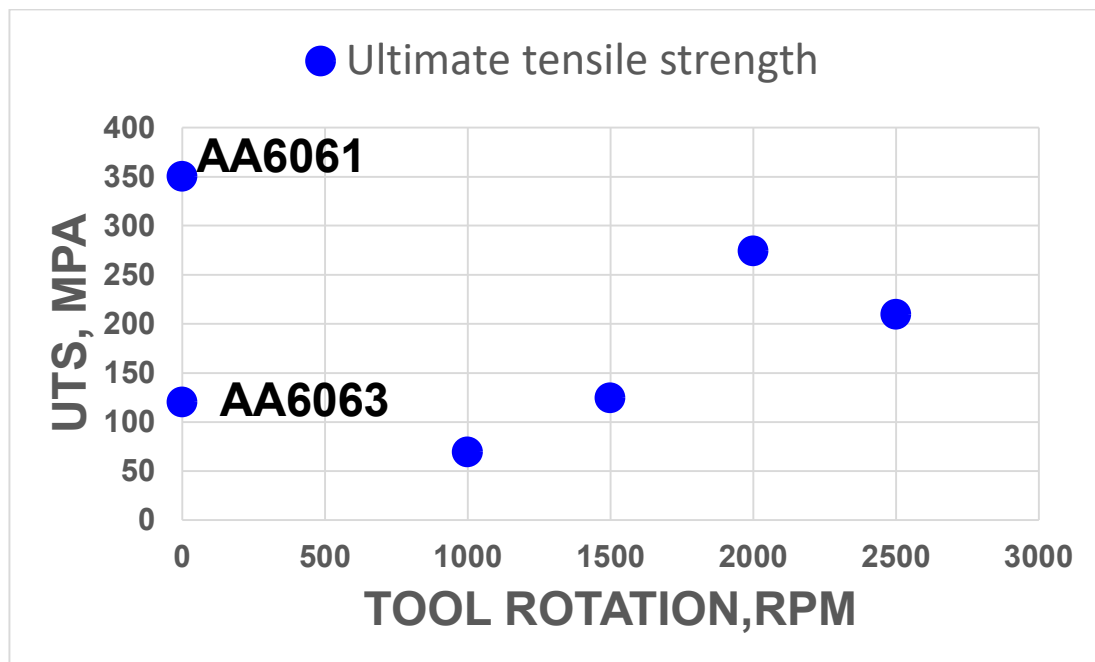
The total elongation of the base alloys and weldments at 2000 and 2500 rpm are found to be almost similar ($\sim 20\%$). However, the extent of total elongation is found to be order of 5 – 15 %, which might be associated to the presence of porosity in the weldment fabricated at 1000 and 1500 rpm. On the other hand, the YS and UTS of the weldments is found to increase with the increase in the rotational speed. As observed during the visual examination of the weldments, the extent of porosity associated with the FSW is found to decrease with increase in the rotational speed of FSW process. The porosity is found to be completely absent in the weldment fabricated at the rotational speed of 2000 and 2500 rpm. As a result, the YS and UTS of the weldment at 2000 rpm is found to be at maximum level. However, the strength of the weldment at 2500 rpm is found to lower, which is ascribed to the heat generation of during FSW process. The amount heat generation during FSW process is directly proportional to the rotational speed of the FSW process. The highest of the heat is expected to be generated during FSW process with a rotational speed of 2500 rpm. The heat might have caused the coarsening of the precipitates, softening of the weldment and microstructural damage of the heat affected zone (HAZ), which in turn lowers the strength of the weldment at 2500 rpm.

Figure 5.1: Tensile properties of the base and weldments at room temperature

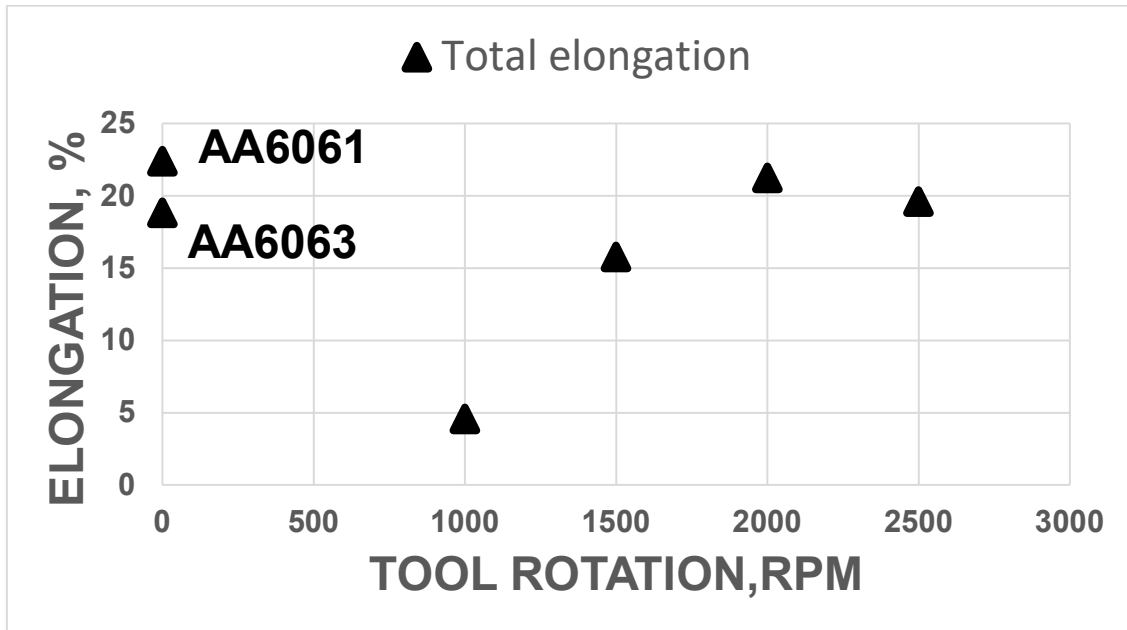
Description	BASE AA 6061	BASE AA 6063	FSW -W1	FSW -W2	FSW -W3	FSW -W4
UTS Stress,MPa	350.00	120.00	69.00	124.37	273.86	209.60
Yield Stress, MPa	233.33	78.9	51.2	82.9	183	140
Total Elongation %	18.82	22.39	4.58	15.78	21.24	19.6
RPM	0	0	1000	1500	2000	2500



a)



(b)



(c)

Figure 5.4: Variation of (a) Yield strength, (b) Ultimate tensile strength and (c) Total elongation against Tool Rotation of Base AA 6061, AA 6063 and Friction Stir welded samples Rotation.

5.3 Microstructural Analysis:

The tool rotation speed has a significant impact on the microstructure grain size at different region of the weld. The base material of AA6061 alloy was forged and extruded, whereas the base AA6063 alloy was received in the form of a cast product. In the present investigation, the microstructures of the base AA6061 and AA6063 alloys and FSW weldment fabricated at a rotational speed of 2000 rpm are shown at different magnifications in Figures 5.4 through 5.6. As the weldment produced at 2000 rpm has shown the highest amount of strength and ductily among all weldments fabricated at different rotational speed, the microstructure of the weldment at 2000 rpm has been investigated. The The EDS spectra of the precipitates present in the base alloys and weldment produced at 2000 rpm are revealed in Figures 5.7 through 5. 9.

Based on the SEM investigation, the following findings are made:

1. The base AA6061 alloy has a equiaxed grain structure. Furthermore, it has limited precipitates within the matrix.
2. The presence of grain is completely absent in the base AA6063 alloy. However, a significant amount of precipitates are noticed in the matrix of the alloy.
3. The weldment fabricated at 2000 rpm has revealed a limited presence of grain boundary. The significant presence of precipitates are identified within the matrix of weldment.
4. The grain boundaries at the weldments appears to be serrated in nature.
5. The EDS analyses have confirmed the occurrence of Mg_2Si precipitates in the base alloys and weldment, which promotes precipitation hardening in the alloy.

As the base AA6061 was forged and extruded, the presence of equiaxed grain is found as expected. The grain boundary is identified to be absent in the base AA6063 alloy, owing to as-cast structure. In the weldment, the tool rotational speed in FSW causes churning and mixing of material around the spinning pin, which in turn causes the changes in the microstructure of the weldment. As a consequence, a few grain boundaries are noticed in the weldment. The mechanical properties of any materials are governed by the microstructure, i.e., grain size and precipitate formation. According to the Hall-Petch relation, the fine grain structure promotes the strength in a material. Therefore, the fine grain structure of the base AA6061 alloy has promoted superior tensile property of the alloy among all conditions. The strength of the base AA6063 alloy is lower due to the absence of the grain boundary. The strength of the weldment fabricated at 2000 rpm has intermediate strength owing to the limited grain boundaries

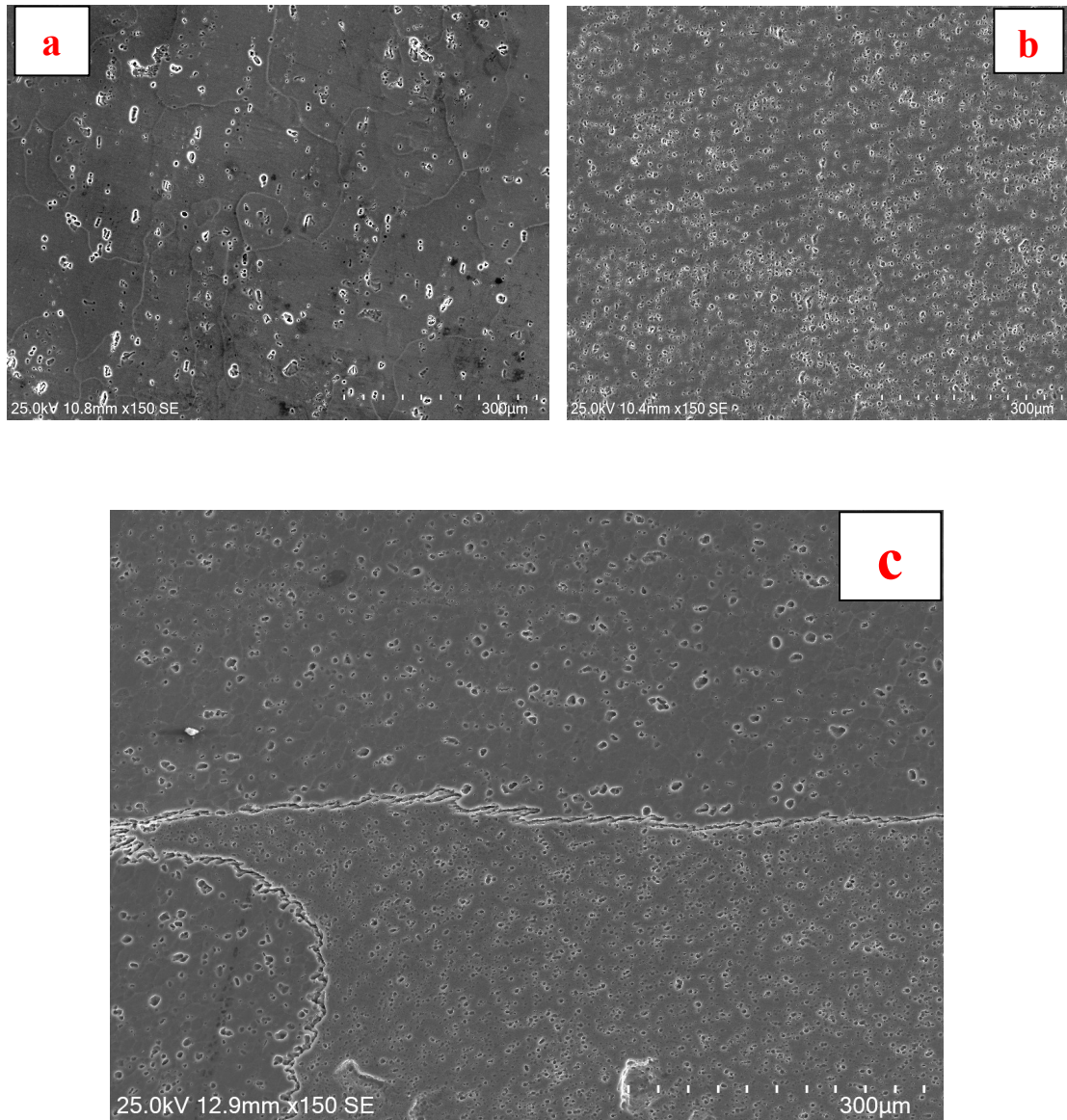


Figure 5.5: Microstructure Base(a) AA 6061, (b) AA 6063 and (c)Friction Stir welded sample with 2000 Tool Rotation at magnification 150X.

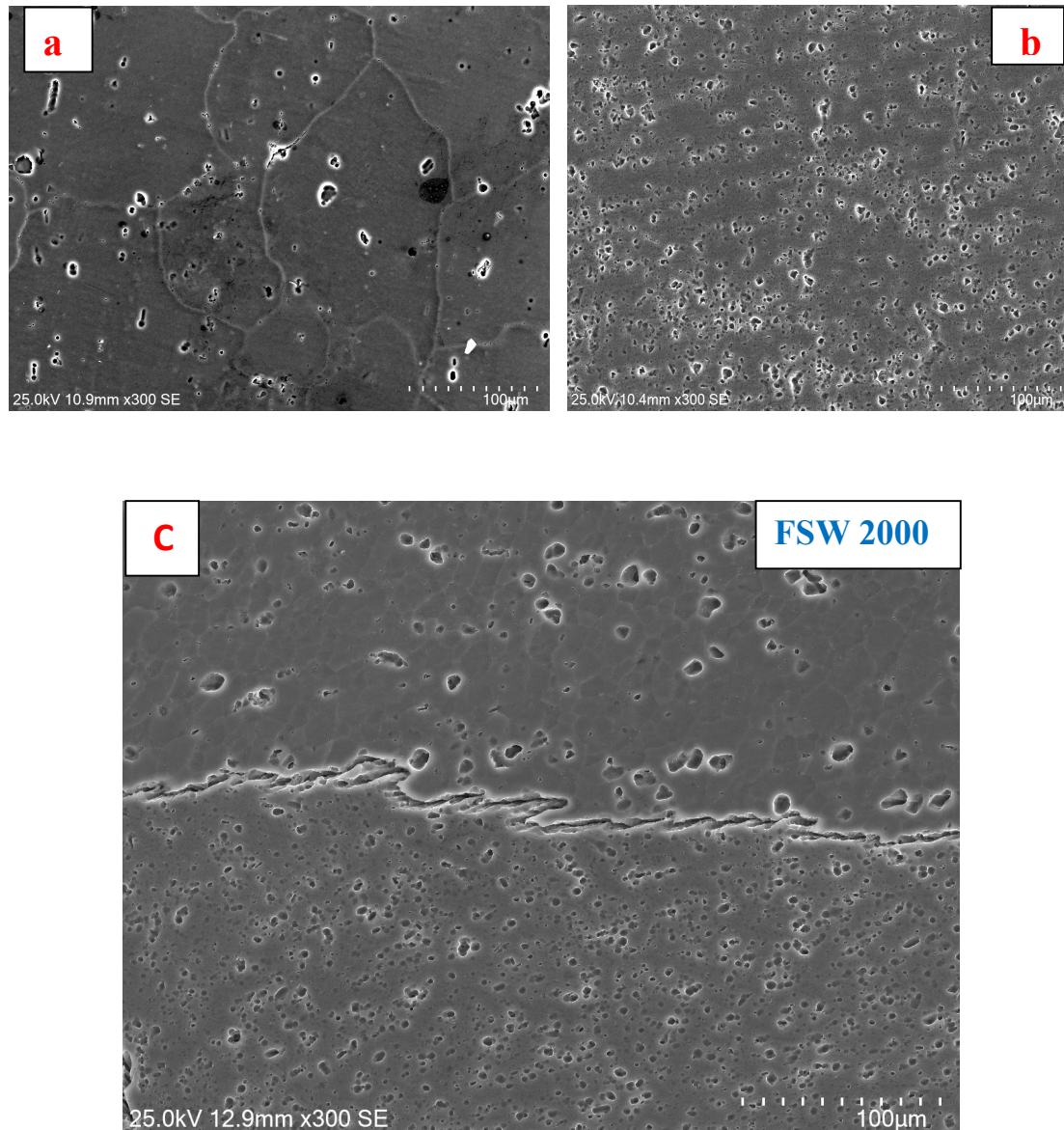


Figure 5.6: Microstructure Base(a) AA 6061, (b) AA 6063 and (c)Friction Stir welded sample with 2000 Tool Rotation at magnification 300 X.

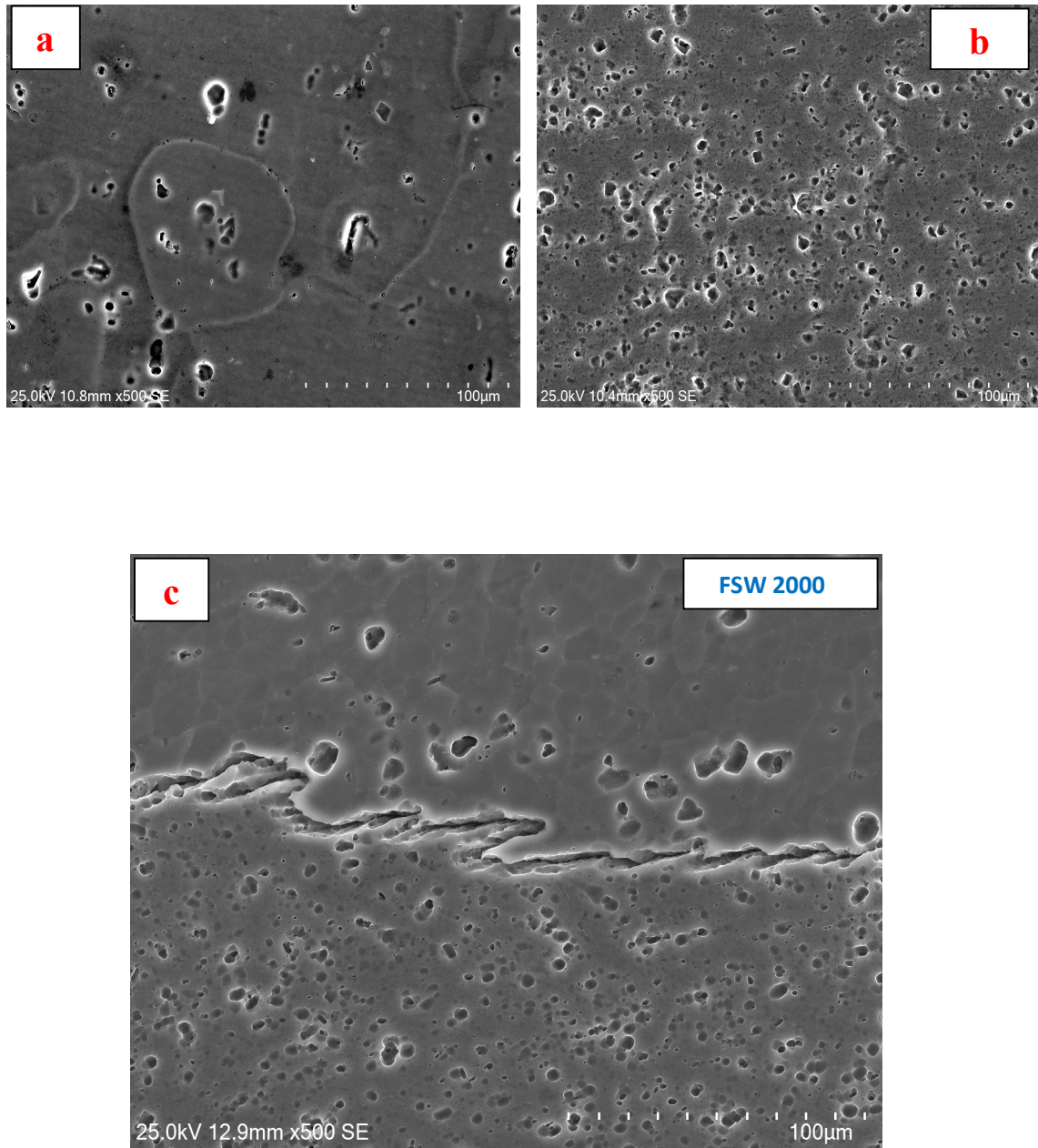
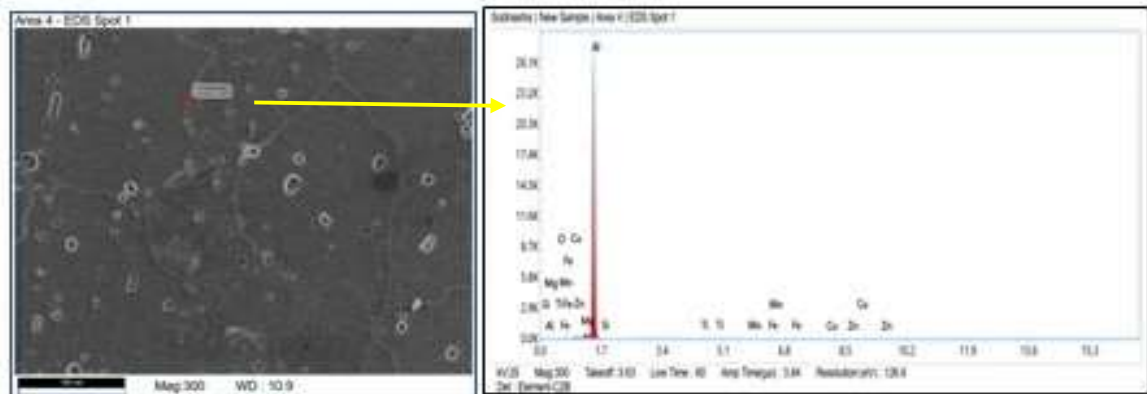


Figure 5.7: Microstructure Base(a) AA 6061, (b) AA 6063 and (c)Friction Stir welded sample with 2000 Tool Rotation at magnification 500X.

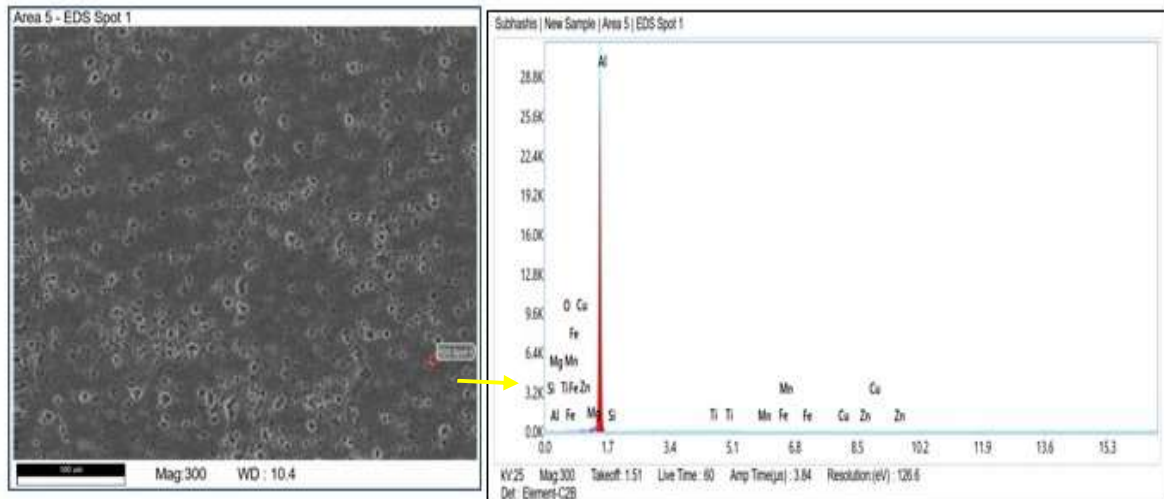
Sample Name: Base AA6061



Element	Weight %	Atomic %	Error %	Net int.	R	A	F
O K	0.75	1.27	39.32	2.13	0.8919	0.0258	1.0000
Mg K	2.43	2.69	10.19	81.52	0.9095	0.2939	1.0514
Al K	94.87	94.78	7.22	3617.13	0.9134	0.3750	1.0015
Si K	0.70	0.67	30.08	4.36	0.9171	0.0631	1.0020
Ti K	0.18	0.10	32.94	4.66	0.9416	0.6424	1.0295
Mn K	0.27	0.13	29.56	6.29	0.9494	0.8119	1.0580
Fe K	0.26	0.12	21.88	5.84	0.9519	0.8494	1.0699
Cu K	0.34	0.15	26.14	6.04	0.9593	0.9211	1.1213
Zn K	0.20	0.08	32.53	3.15	0.9618	0.9367	1.1431

Figure 5.8: Chemical composition element of particles done by EDX spectra of base 6061 Al alloys.

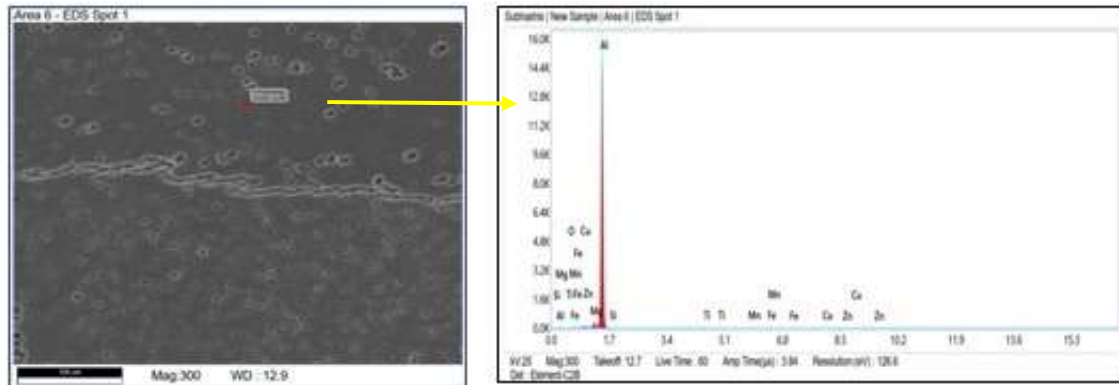
Sample Name: BASE AA 6063



Element	Weight %	Atomic %	Error %	Net Int.	R	A	F
O K	0.60	1.01	40.82	1.69	0.8921	0.0257	1.0000
Mg K	1.48	1.64	10.60	50.99	0.9097	0.3022	1.0563
Al K	96.82	96.71	6.92	3960.54	0.9136	0.4034	1.0014
Si K	0.23	0.22	73.06	1.42	0.9173	0.0626	1.0020
Ti K	0.19	0.11	32.55	4.94	0.9417	0.6416	1.0286
Mn K	0.14	0.07	55.41	3.17	0.9495	0.8114	1.0572
Fe K	0.19	0.09	25.26	4.22	0.9520	0.8491	1.0691
Cu K	0.19	0.08	45.93	3.30	0.9595	0.9217	1.1228
Zn K	0.17	0.07	47.07	2.66	0.9620	0.9372	1.1452

Figure 5.9: Chemical composition element of particles done by EDX spectra of base Al 6063 alloys.

Sample Name: FSW Dissimilar Al Alloys (AA6061 & AA6063)



Element	Weight %	Atomic %	Error %	Net Int.	R	A	F
O K	1.05	1.77	40.98	1.72	0.8917	0.0258	1.0000
Mg K	2.39	2.65	10.78	45.28	0.9094	0.2869	1.0501
Al K	94.15	94.02	7.34	2047.75	0.9133	0.3692	1.0015
Si K	0.88	0.84	32.53	3.20	0.9170	0.0634	1.0021
Ti K	0.32	0.18	21.15	4.68	0.9415	0.6430	1.0296
Mn K	0.26	0.13	36.68	3.49	0.9493	0.8116	1.0587
Fe K	0.25	0.12	30.15	3.25	0.9518	0.8492	1.0710
Cu K	0.49	0.21	23.91	4.96	0.9593	0.9210	1.1203
Zn K	0.23	0.09	33.85	2.09	0.9618	0.9365	1.1418

Figure 5.10: Chemical composition element of particles done by EDX spectra of FSW weldment at tool rotation 2000 RPM..

5.4 Fractography:

FSW was used to successfully combine two high strength dissimilar aluminum alloys (AA6061 and AA6063).

Scanning electron fractographic features of the tensile-tested samples of the specimen (AA 6061, AA 6063 and FSW weldment at 2000 RPM) is shown in Figures 5.10 through 5.13 to understand the operating failure mechanism.

The base alloys have a significant amount of ductility (~20% total elongation). Therefore, the base alloys has shown the presence of the dimple fracture surfaces, which is a characteristic feature of the ductile failure. During tensile deformation of base alloy, the voids are nucleated at the interface of the precipitates and matrix. These voids grow further during tensile deformation, and coalesce each other, which in turn produces dimple fracture surface, as depicted Figure 5.10 through 5.13. Furthermore, the number density of the dimples is found to be higher in the AA6063 alloy, which is owing to enhanced presence of the precipitates in the alloy as shown in Figures 5.4 through 5.6. Moreover, the size of the dimples is found to be smaller in the tensile-tested samples of AA6063 alloy. The enhanced presence of precipitates in the AA6063 alloy has led to formation of significant number of nucleation sites of voids. The dominance of nucleation of voids over the growth of the voids during tensile deformation of the AA6063 alloy has caused small sized dimples and higher number density of voids of the AA6063 alloy. In contrast, the presence of precipitates are found to be lower in the AA6061 alloy. The limited occurrence of the precipitates has caused the dominance of growth of voids over the nucleation of the void. As a results, the number density of the voids are found to be lower, and the size of the dimple appears to be coarser in the AA6061 alloy. On

the other hand, the tensile-tested sample of FSW weldment has revealed the occurrence of cleavage facets in the fracture surface.

The welded joint fractures at its weakest point, which is located in the softer part of the joint. The tensile specimen was shattered from the HAZ of the softer material (AA6063) side.

Because of the heat cycle, the weakest zone has big grain size and coagulated precipitates. Fractography in the mid-section of the fractured sample, shown in Figures 5.10 through 5.13 at different magnifications, to describe the fracture mechanism of the joint. The tensile specimens was broken by the cracking of large-sized coagulated precipitates situated along the HAZ of AS. Fine dimples were first produced during precipitation breaking, which was then followed by precipitation breaking. The strength of the joints is significantly influenced by the size of the strengthening precipitates. Smaller precipitates have slower dislocation motion, which strengthens the material. Massive precipitates, on the other hand, ineffectively impede dislocation motion, leading to precipitate cracking.

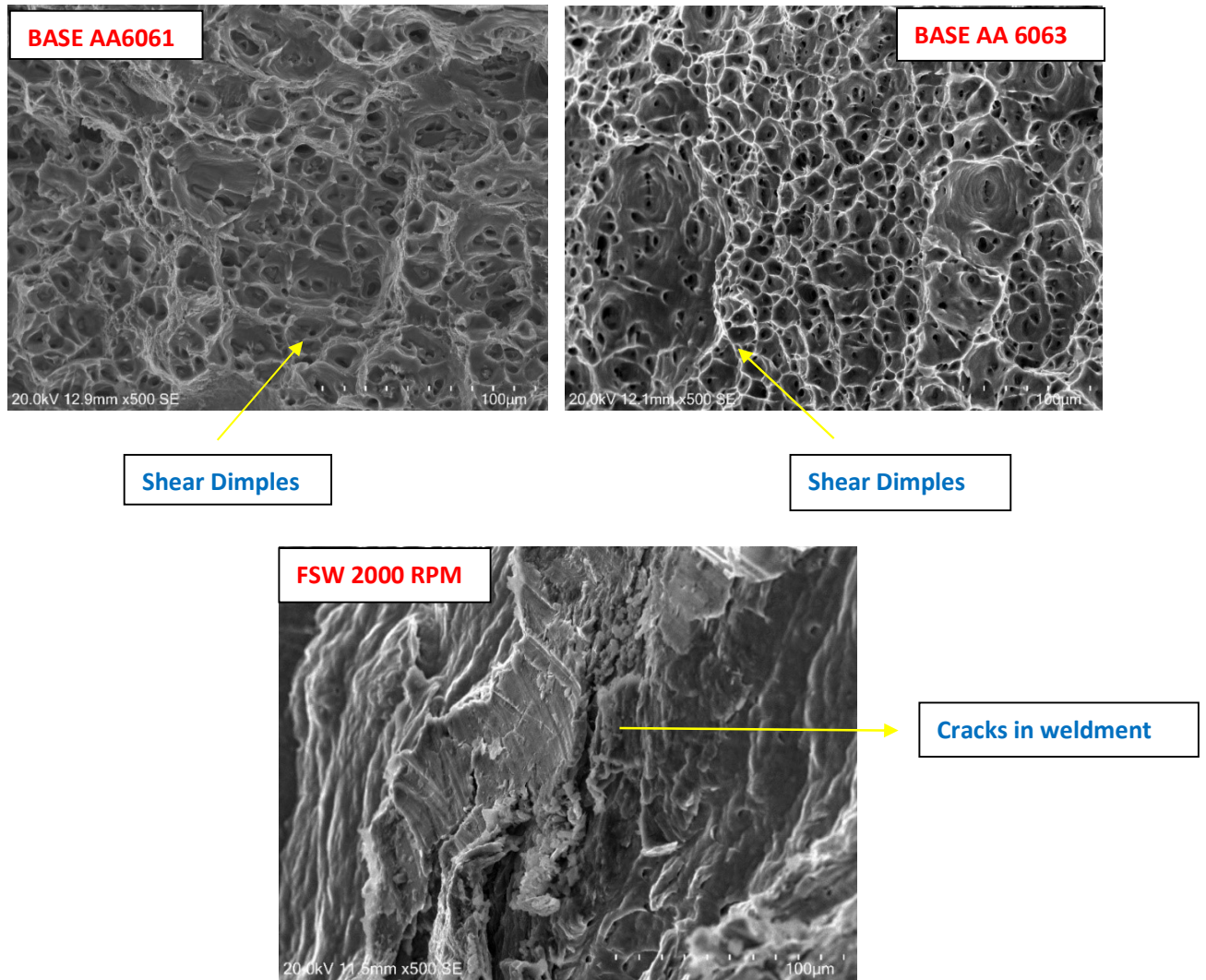


Figure 5.11: Tensile Fractography Base AA 6061, AA 6063 and Friction Stir welded sample with various Tool Rotation at 500 X magnification.

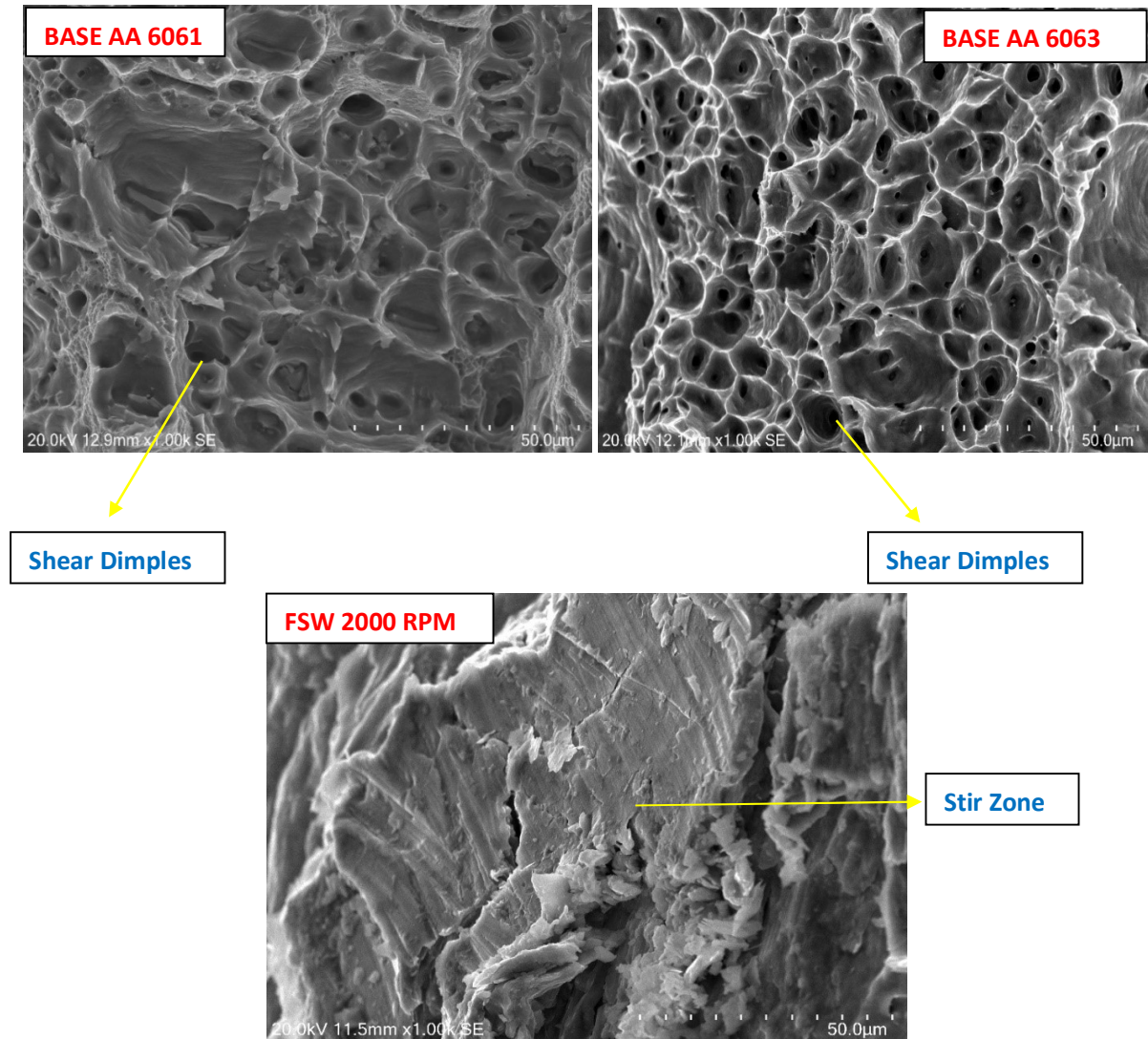


Figure 5.12: Tensile Fractography Base AA 6061, AA 6063 and Friction Stir welded sample with various Tool Rotation at 1000 X magnification.

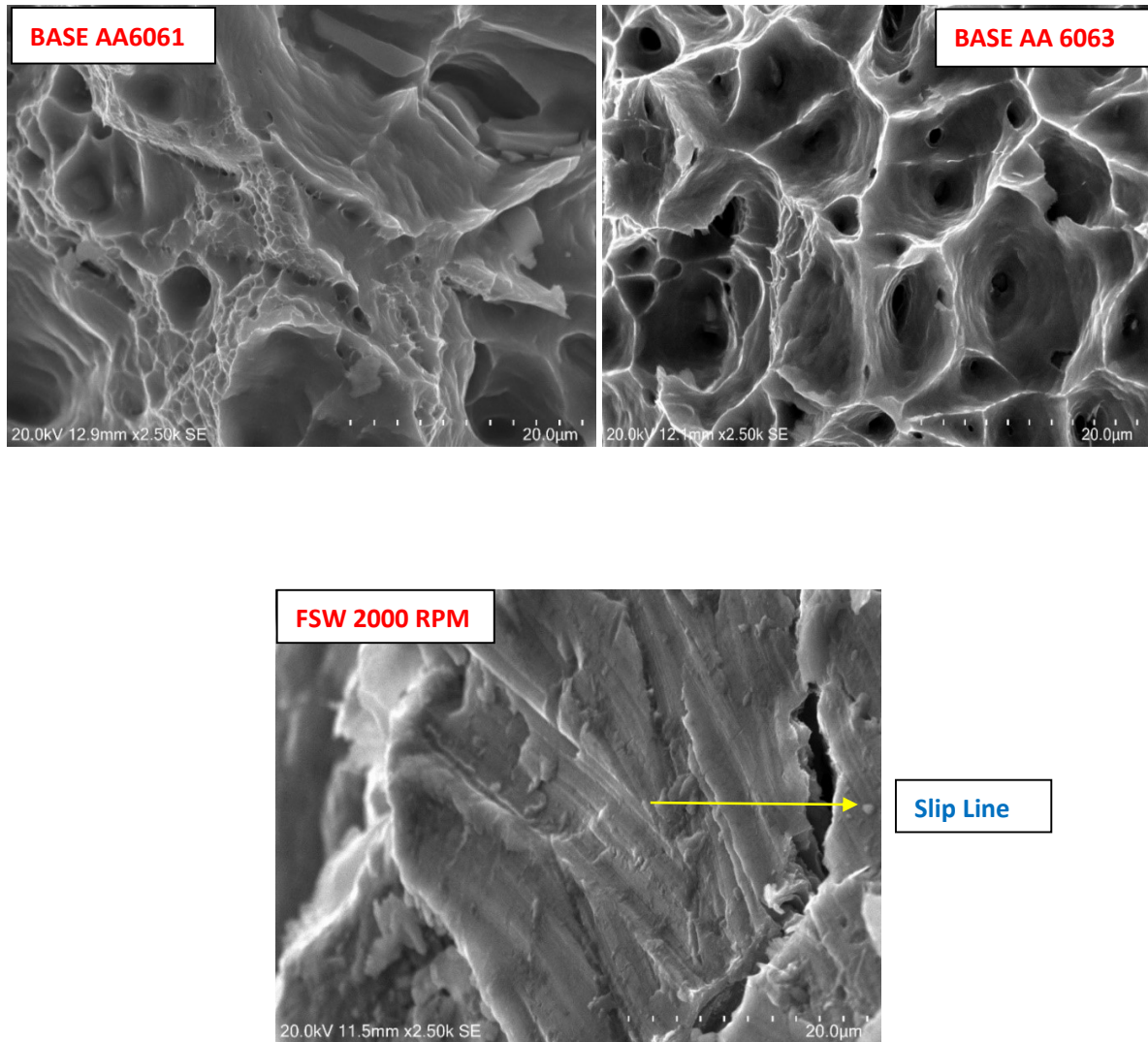


Figure 5.13: Tensile Fractography Base AA 6061, AA 6063 and Friction Stir welded sample with various Tool Rotation at 2500 X magnification.

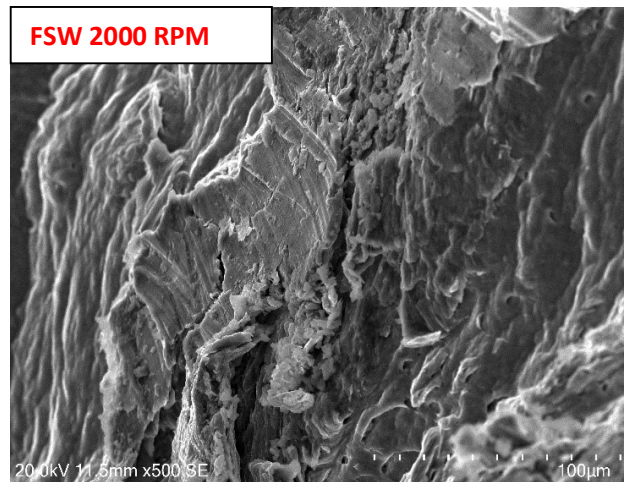
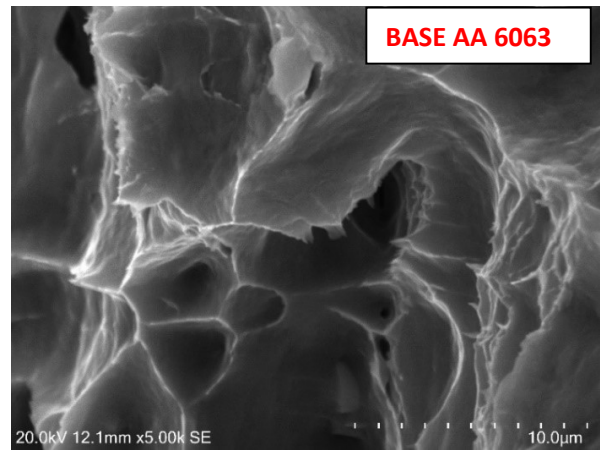
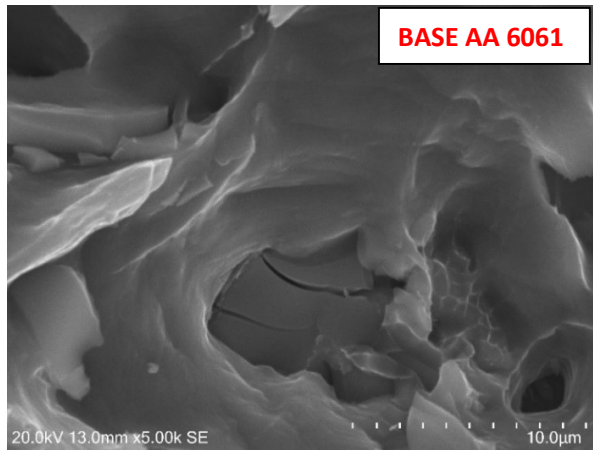


Figure 5.14: Tensile Fractography Base AA 6061, AA 6063 and Friction Stir welded sample with various Tool Rotation at 5000 X magnification.

5.5 Micro Hardness:

Figure shows the micro hardness values for friction stir welded specimens. The parent metal's hardness was roughly 28 HV (AA 6063 alloy) and 76 HV (AA 6061 alloy). The hardness of the stir zone varied according to position, ranging from 68 to 70 HV. The hardness value of the friction stir welded zone is higher than that of the base AA6063 alloy, but lower than the base AA6061 alloy.

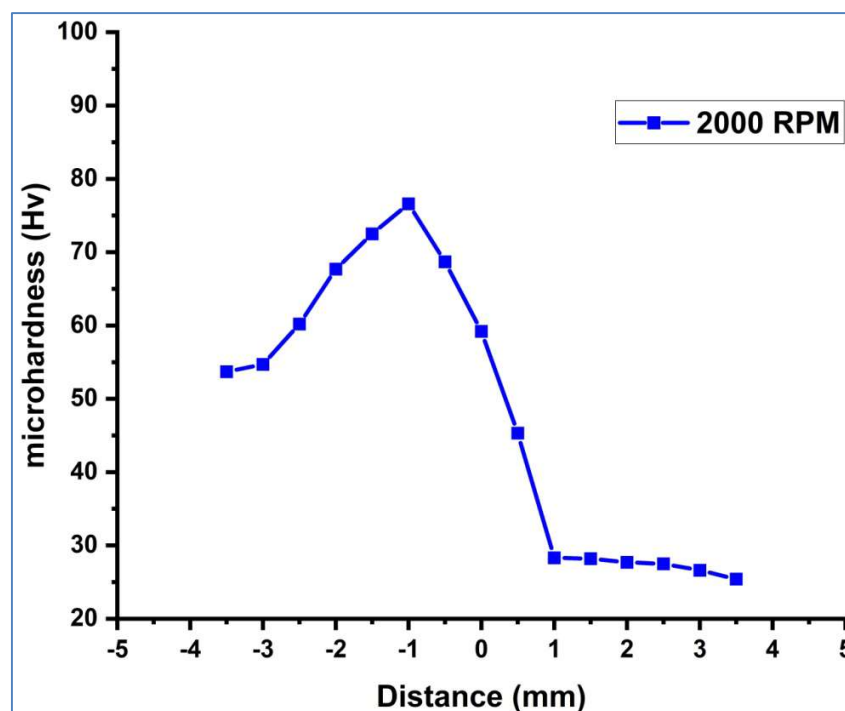


Figure 5.15: Micro Hardness (HV) vs distance plot of Base AA 6061, AA 6063 and Friction Stir welded sample with 2000 RPM Tool Rotation

Generally, two variables, grain size and occurrence of precipitates contribute to the enhanced hardness of the friction stir zone. Grain refinement is a vital in material strengthening. As the grain size of the friction stir zone is much finer than that of the AA6063 alloy, the hardness of the friction

stir zone is found to be higher. Secondly, the occurrence of the precipitates in the friction stir zone and base AA6063 alloy is found to be comparable. Therefore, in the present investigation, only the grain size has a significant role on the hardness of the weldment and base metal. The hardness of the base AA6061 alloy has highest hardness owing to the relatively fine grain-structure among all conditions.

5.6 Corrosion Resistance Analysis

As seen in the picture, the fundamental materials were considerably impacted by all corrosive conditions. The weld area surface, on the other hand, was slightly degraded, indicating that the weld region specimen had good corrosion resistance. Except for the seawater medium, all of the submerged surfaces were changed to a whitish tint. The seawater medium developed an ash-colored corrosion coating on the specimens' submerged surfaces, providing good corrosion resistance. Both salt spraying and submersion studies were used to calculate weight loss. Based on the weight loss, Equation (1) was used to calculate the corrosion rate (mm/yr). Submersion test media and their details as per table 5.2

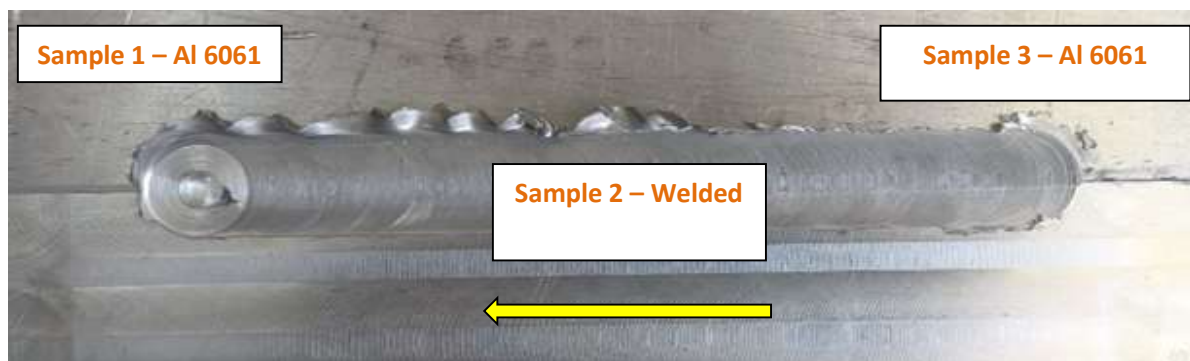
Sl No	Solution	pH Value	Temp ° C	Submersion Time (Days/Hour)
1	3.5% wt HCL +H ₂ O	3.08	32	12/288
2	3.5% wt H ₂ SO ₄ +H ₂ O	3.51		
3	Sea Water (3.5% wt NaCl)	7.52		

Fontana's mathematical formula for determining corrosion rates of samples following weight loss measurement is as follows:

$$CR = 87.6 W/AT \text{ (mm/yr) } \dots\dots\dots(1)$$

where CR = corrosion rate in millimeters per year, w = weight loss in mg, this was done by subtracting the final weight measured from the initial weight, which gave the weight loss (weight difference),

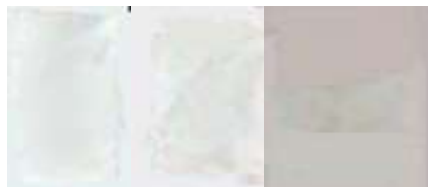
A = Area, the area of each sample was determined by calculating the total surface area in cm², and T = Time, this was an exposure time in hours that each of the samples spent inside the different concentrations of acidic media.



RPM –2000 RPM & FEED 60 mm/min



**Al 6061 Base Metal after
Corrosion Testing**



**FSW Welded Sample
after Corrosion Testing**



**Al 6063 Base Metal after
Corrosion Testing**

After Submerge d in 3.5% HCL+H ₂ O	After Submerged in 3.5% H ₂ SO ₄ +H ₂ O	After Submerged in 3.5% NaCl
--	---	------------------------------------

Figure 5.14: Corrosion Testing in 3 diff type solution of Base AA 6061, AA 6063 and Friction Stir welded sample with 2000 Tool Rotation.

As seen in the image, all corrosive conditions had a considerable impact on the base materials. The weld area surface, on the other hand, was slightly degraded, indicating that the weld region specimen had good corrosion resistance. Except for the seawater medium, all of the submerged surfaces were changed to a whitish tint. The seawater medium developed an ash-colored corrosion coating on the specimens' submerged surfaces, providing good corrosion resistance. The laboratory submersion test findings are presented in terms of sample weight before and after submersion, weight loss due to corrosion solutions, and Cr levels for each specimen.

The Corrosion Test at various medium are shown below in Table 5.3

Sl No	Material	Solution	Weight of the Sample before Submersion(g) Wb	Weight of the Sample after Submersion(g) Wb	Weight Loss(g) ΔW	Corrosion Rate(m mYr) Cr
1	AA 6063	3.5% wt HCL +H2O	11.5	9.772	1.728	0.0433
2	AA6061	3.5% wt HCL +H2O	11.52	9.554	1.966	0.0488
3	FSW Sample	3.5% wt HCL +H2O	11.42	9.776	1.644	0.0411
4	AA 6063	3.5% wt H2SO4 +H2O	11.5	9.86	1.64	0.0411
5	AA6061	3.5% wt H2SO4 +H2O	11.51	9.71	1.8	0.0449
6	FSW Sample	3.5% wt H2SO4 +H2O	11.42	9.956	1.464	0.0366
7	AA 6063	Sea Water (3.5% wt NaCl)	11.5	11.218	0.282	0.0071
8	AA6061	Sea Water (3.5% wt NaCl)	11.51	11.216	0.294	0.0073
9	FSW Sample	Sea Water (3.5% wt NaCl)	11.42	11.216	0.204	0.0051

The results of the submersion test indicated that acid media such as HCl and H2SO4 are more corrosive than alkaline media such as saltwater. H2SO4 was more corrosive than HCl among the acid media tested here. The weld region specimen had the highest CR values in every test medium.

For all three specimens studied, weight loss in the weld zone was low, ranging from 1.644 g (HCl) to 1.464 g (H₂SO₄) under acid circumstances and up to 0.204 g in alkaline media (seawater).

Weight loss of in acid media ranged from 1.728 g (HCl) to 1.64 g (H₂SO₄), whereas in alkaline media (seawater) the values ranged from 0.282 g (Al6061) to 0.294 g (Al6063).

The CR values after 12 days of immersion in three different solutions for the base material and weld zone specimens. CR values for base materials in acid solutions ranged from 0.0448 mm/yr (HCl) to 0.0449 mm/yr (H₂SO₄), whereas CR values in saltwater ranged from 0.0071 mm/yr (AA6063) to 0.00733 mm/yr (Al6061).

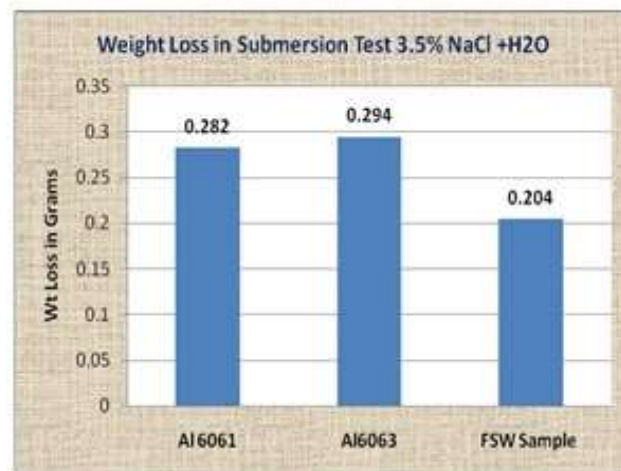
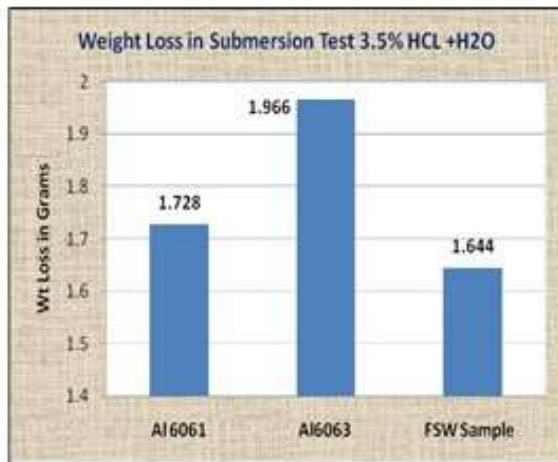


Figure 5.15: Weight Loss Chat Base AA 6061, AA 6063 and Friction Stir welded sample with 2000 RPM Tool Rotation (a) 3.5 % HCL +H₂O (b) H₂SO₄ +H₂O (C) 3.5% NaCl Solution



Figure 5.16: Corrosion rate Chat Base AA 6061, AA 6063 and Friction Stir welded sample with 2000 RPM Tool Rotation (a) 3.5 % HCL +H₂O (b) H₂SO₄ +H₂O (C) 3.5% NaCl Solution

Although the grain sizes of the basic materials were uniform, they changed throughout the rolling process, resulting in dislocation flaws. When base materials are regularly intermixed during welding, recrystallization produces homogeneous equiaxed grains. Recrystallization of grains improves mechanical and thermal properties, as well as the number of flaws in the weld zone, which has a greater CR. Recrystallization occurs in the weld region of similar alloys, but this does not provide cathodic protection, resulting in poorer corrosion resistance in the weld regions of dissimilar alloys. Furthermore, seawater can raise CR values, making base metals more prone to metal loss.

The weight loss rates were greater in the base materials (AA6061 and AA6063) than in weld area specified in all submission media, demonstrating that denser grain induce higher CR.

Using the FSW approach, the corrosion behaviors of two dissimilar alloys (AA6061 and AA6063) were examined under various corrosion situations that represented marine applications.

In submersion testing, the weight loss at the weld site was significantly less than for the basic materials Al6061 and Al6063. The samples were immersed in seawater, 3.5 weight percent H₂SO₄ solution, and 3.5 weight percent HCl solution for a total of 12 days. Seawater and HCl solutions had the lowest corrosion rates, respectively, and H₂SO₄ solution had the highest. It was discovered that the Corrosion Resistant in the weld zone was higher than that of the base materials (Al6061 and Al6063).

CHAPTER -6

CONCLUSIONS AND FUTURE SCOPE OF WORK

6.1Conclusions:

1. Dissimilar Aluminium Alloy 6061 and 6063 friction stir welding was successfully completed with a constant welding speed, variable tool rotation rates, and a tapered conical pin profile tool. Among four plates, the best joint of friction stir welding of dissimilar Aluminium Alloy 6061 and 6063 is at a tool rotational speed of 2000 rpm and a welding speed of 60mm/min. Tensile testing revealed that sample , which was welded at a low rotational speed (2000 rpm), had the highest tensile strength (183 MPa). This is because when tool rotating speed increases, coarse grain structure is formed, resulting in poor ultimate tensile strength.
2. The% Elongation is greater for samples welded at rotating speeds of 2000rpm and 2500rpm than less for rotational speeds of 1000rpm and 1500rpm. At a tool rotation speed of 2000rpm, the threaded pin profile tool is at its best having elongation 21.24%.
3. SZ has smaller grain size than other zones due to intense plastic deformation, which resulted in grain refinement produced by dynamic recrystallization of the material being welded. TMAZ has a greater grain size than SZ because it undergoes partial dynamic recrystallization due to a lack of heat and deformation required for complete recrystallization. HAZ has bigger grain size than the other two zones since it only encounters heat cycles with no plastic deformation. The mechanical properties of welded joints are governed by the microstructure (grain size and precipitate formation) of the joint.
4. The joint's surface morphology was flawless, with no imperfections. Joint was broken by the advancing side's HAZ. The weakest zone with big particle size was discovered to be the HAZ. On the shattered surface, shear dimples and densely packed fine dimples were seen.

6.2 Future Scope of Work:

1. As a scope of future work, apart from tensile testing and microstructural examination, other mechanical tests such as fatigue testing could also be performed to get the better understanding of the fracture behaviour of the welded joints.
2. Attempts will be made in the future to produce Al-based nanocomposites using the Friction Stir Welding (FSW) technique. Al₂O₃ nanoparticles were incorporated into the aluminum matrix to refine the microstructure of the nugget zone (NZ) and to limit granular development in the heat-affected zone (HAZ). The effects of Al₂O₃ nanoparticles on the grain structure evolution and various mechanical properties of a friction stir welded aluminum matrix will be investigated.

References:

- [1] Fu Zhi-Hong, He Di-Qiu; Wang Hong, Friction Stir Welding of Aluminum Alloys, Journal of Wuhan Univ. of Tech. Vol. 19, No.1 (2004) page 61-64.
- [2] Thomas WM, Nicholas ED, Needham JC, Murch MG, Templesmith P, Dawes CJ, G B Patent Application No.9125978.8; December 1991.
- [3] Mishra RS, Ma ZY. Friction stir welding and processing. Mater Sci Eng 2005;R50: 1–78.
- [4] T. Nagasawa, M. Otsuka, T. Yokota, T. Ueki, in: H.I. Kaplan, J. Hym, B. Clow (Eds.), Magnesium Technology 2000, TMS, 2000, pp. 383–386.
- [5] M.C. Juhas, G.B. Viswanathan, H.L. Fraser, in: Proceedings of the Second Symposium on Friction Stir Welding, Gothenburg, Sweden, June 2000.
- [6] W.B. Lee, S.B. Jung, The joint properties of copper by friction stir welding, Mater. Lett. 58 (2004) 1041–1046.
- [7] Kallee, S.W. (2006-09-06). "Friction Stir Welding at TWI". The Welding Institute (TWI). Retrieved 2009-04-14.
- [8] Seidel, TU; Reynolds, AP (2001). "Visualization of the Material Flow in AA2195 Friction-Stir Welds Using a Marker Insert Technique". *Metallurgical and Material Transactions* 32A (11): 2879–2884.
- [9] M.J. PEEL, A. STEUWER, P.J. WITHERS, T. DICKERSON, Q. SHI, and H. SHERCLIFF, “Dissimilar Friction Stir Welds in AA5083-AA6082. Part I and II: Process Parameter Effects on Thermal History and Weld Properties”. *Metallurgical and Materials Transaction A*, Vol. 37A, July 2006-2183-2206.

- [10] K. Elangovan, V. Balasubramanian, "Influences of tool pin profile and tool shoulder diameter on the formation of friction stir processing zone in AA6061 aluminium alloy", *Materials and Design* 29 (2008) 362-373.
- [11] Hidetoshi Fujii , Ling Cui, Masakatsu Maeda, Kiyoshi Nogi, Effect of tool shape on mechanical properties and microstructure of friction stir welded aluminum alloys, *Material Science and Engineering A* 419 (2006) 25-31.
- [12] R.Palanivel, Dr. P. Koshy Mathews, Dr. N. Murugan. Influences Of Tool Pin Profile On The Mechanical And Metallurgical Properties Of Friction Stir Welding Of Dissimilar Aluminum Alloy, *International Journal of Engg. and Tech.* Vol. 2 (6), 2010, 2109-2115.
- [13] T. Hirata , T. Oguri , H. Hagino , T. Tanaka , S. Chung , Y. Takigawa , K. Higashi , *Materials Science and Engineering : A*, 456 (2007) 1-2 ,344.
- [14] H. Lombard, D. Hattingh, A. Steuwer, M. James, Optimizing FSW Process Parameters To Minimise Defects And Maximise Fatigue Life in 5083-H321 Aluminium Alloy, *Engineering Fracture Mechanics*, (2013), 75 (3–4), 297-900.
- [15] Afsal.A.Kareem, The Influence Of Stirrer Geometry On Bonding And Mechanical Properties In Friction Stir Welding Process, *Materials & Design*, 25(2013): 343-347.
- [16] M.S.Srinivasa Rao, B.V.R.RaviKumar.Manzoor Hussain, Experimental study on the effect of welding parameters and tool pin profiles on the IS:65032 aluminum alloy FSW joints, *Materials Today: Proceedings* 4 (2017) 1394–1404.
- [17] www.egr.msu.edu/~pkwon/me477/welding.pdf. PART VII JOINING & ASSEMBLY PROCESSES FUNDAMENTALS OF WELDING.

END